


2018

An optimization and uncertainty quantification framework for patient-specific cardiac modeling

Joshua Mineroff
Iowa State University

Follow this and additional works at: <https://lib.dr.iastate.edu/etd>

 Part of the [Art and Design Commons](#), and the [Mechanical Engineering Commons](#)

Recommended Citation

Mineroff, Joshua, "An optimization and uncertainty quantification framework for patient-specific cardiac modeling" (2018). *Graduate Theses and Dissertations*. 17269.

<https://lib.dr.iastate.edu/etd/17269>

This Dissertation is brought to you for free and open access by the Iowa State University Capstones, Theses and Dissertations at Iowa State University Digital Repository. It has been accepted for inclusion in Graduate Theses and Dissertations by an authorized administrator of Iowa State University Digital Repository. For more information, please contact digirep@iastate.edu.

**An optimization and uncertainty quantification framework for
patient-specific cardiac modeling**

by

Joshua Mineroff

A dissertation submitted to the graduate faculty
in partial fulfillment of the requirements for the degree of
DOCTOR OF PHILOSOPHY

Major: Mechanical Engineering

Program of Study Committee:
Adarsh Krishnamurthy, Co-major Professor
Baskar Ganapathysubramanian, Co-major Professor
Ming-Chen Hsu
James Oliver
Judy Vance

The student author, whose presentation of the scholarship herein was approved by the program of study committee, is solely responsible for the content of this dissertation. The Graduate College will ensure this dissertation is globally accessible and will not permit alterations after a degree is conferred.

Iowa State University

Ames, Iowa

2018

Copyright © Joshua Mineroff, 2018. All rights reserved.

DEDICATION

To my partner, Brittany Tawes. Without your incredible love and support this dissertation would never have been completed. Thank you for everything.

TABLE OF CONTENTS

LIST OF TABLES	v
LIST OF FIGURES	vii
ACKNOWLEDGEMENTS	x
ABSTRACT	xi
CHAPTER 1. INTRODUCTION	1
CHAPTER 2. OPTIMIZATION FRAMEWORK FOR PATIENT-SPECIFIC CAR-	
DIAC MODELING	6
2.1 Abstract	6
2.2 Acknowledgements	7
2.3 Introduction	8
2.4 Related Work	10
2.5 Methods	12
2.5.1 Optimization framework	12
2.5.2 Clinical data	14
2.5.3 Circulation model	15
2.5.4 Finite-element model	20
2.6 Results	22
2.6.1 Circulation model results	22
2.6.2 Finite-element model results	28
2.7 Discussion	30

2.8	References	32
2.9	Appendix: Supplemental Methods and Validation	37
CHAPTER 3. OPTIMIZATION FRAMEWORK FOR PATIENT-SPECIFIC MOD-		
	ELING UNDER UNCERTAINTY	41
3.1	Abstract	41
3.2	Acknowledgements	42
3.3	Introduction	42
3.4	Framework for Design Under Uncertainty	45
	3.4.1 Probabilistic parameterization and sampling	45
	3.4.2 Surrogate modeling	48
	3.4.3 Optimization framework	50
3.5	Circulatory Model	51
	3.5.1 CircAdapt	51
	3.5.2 Clinical data	52
3.6	Synthetic Examples	53
	3.6.1 Example 1: One unknown probabilistic variable	54
	3.6.2 Example 2: One unknown and one known probabilistic variable	54
	3.6.3 Example 3: Two unknown probabilistic variables and two probabilis- tic outputs	55
3.7	A Real-World Problem Using Patient Data	56
3.8	Discussion	57
3.9	References	60
CHAPTER 4. SUMMARY AND CONCLUSION		
	REFERENCES	66

LIST OF TABLES

Table 2.1	Experimentally measured and reference data for human patients studied in circulatory optimization. Missing measurements were substituted with appropriately scaled reference values. HR = heart rate; q = mean systemic blood flow; QRS = QRS complex duration; D_{aorta} = diameter of aorta; D_{aortic} = diameter of aortic valve; D_{pulm} = diameter of pulmonary artery; D_{mitral} = diameter of mitral valve; V_{wall} = ventricular wall volume; $Pmax_{LV}$ = peak left-ventricular pressure; EDV_{LV} = left-ventricular end-diastolic volume; MRV = mitral regurgitant volume.	16
Table 2.2	Experimentally measured objectives for canine subjects studied in circulatory optimization. All subject models relied largely on reference data. $Pmax_{LV}$ = peak left-ventricular pressure; EDV_{LV} = left-ventricular end-diastolic volume.	17
Table 2.3	Parameters and bounds of the different optimization variables in \mathbf{x} of the circulation model.	18
Table 2.4	Parameters and bounds of coefficients of \mathbf{x} in Eq. 2.9	21
Table 2.5	Optimized parameters and results of human patients and canine subjects studied in circulatory optimization. Bounded optimal parameter values are bolded. Explanation of variables can be found in Table 2.3.	24

Table 2.6	RMSE between both human and canine model and catheter data when either cuff (with or without using the mean values of MAP and Sf_{act}) or catheter pressure is used as an optimization input. . .	28
Table 2.7	Optimized coefficients from Eq. 2.9 and Klotz curve (Klotz et al., 2006) fit for each canine subject.	29
Table 2.8	RMSE between human model and catheter data when either cuff (with or without using the mean values of MAP and Sf_{act} in \mathbf{x}) or catheter pressure is used as an optimization input and when modeled aortic diastolic pressure is optimized against cuff diastolic pressure.	38
Table 3.1	Details and bounds of the different CircAdapt variables affected by \mathbf{x} .	51
Table 3.2	Summary of synthetic examples. In Example 2, the bolded distribution of input X2 is known by the optimizer.	53
Table 3.3	Convergence results of iCDFs for Example 1.	54
Table 3.4	Convergence results of iCDFs for Example 2. The distribution of X2 is exactly known by the optimizer.	56
Table 3.5	Results for the Real-World example.	57

LIST OF FIGURES

Figure 2.1	<p>The geometric parameters and objective metrics used in the circulatory optimization. (A) A schematic of the CircAdapt model highlighting key geometric dimensions of major model components. A subset of the model values directly driven by patient-specific or reference data (Table 2.1) and the parameters used (Table 2.3) are both shown. (B) A typical simulated left ventricular (LV) pressure-volume loop showing all partial objective metrics. Pulm. = pulmonary circulation; Syst. = systemic circulation; LA = left atrium; RA = right atrium; RV = right ventricle; EDV = end-diastolic volume; EDP = end-diastolic pressure.</p>	15
Figure 2.2	<p>A representative example of both mesh states of the finite-element optimization and the resulting EDPVR curve. (A) A converged unloaded and inflated mesh from the simulation showing the change in ventricular shape and volume. (B) A comparison of the precomputed Klotz curve and simulated pressure-volume curve. EDPVR = end-diastolic pressure-volume relationship.</p>	22
Figure 2.3	<p>Left ventricular pressure-volume loops for the eight human patients.</p>	25
Figure 2.4	<p>Left ventricular pressure-volume loops for the four canine subjects.</p>	25

Figure 2.5	Validation of the simulated left ventricular pressure curves for the eight human patients with catheter data after optimizing based on the peak catheter pressure. Gray lines show cuff measurement systolic and diastolic pressures - only catheter pressure was available as the reference for Patient H.	26
Figure 2.6	Validation of the simulated left ventricular pressure curves for the eight human patients with catheter data after tuning the optimized results with the average MAP and Sf_{act} . Gray lines show cuff measurement systolic and diastolic pressures - only catheter pressure was available as the reference for Patient H.	27
Figure 2.7	Validation of the simulated left ventricular pressure curves for the the four canine subjects with catheterized in-vivo pressure data. Gray line shows reference catheter pressure.	27
Figure 2.8	Results from simulated inflations of four canine left ventricles. (A) The final unloaded meshes. (B) Comparison of the optimized simulated pressure-volume curves to the Klotz curves (Klotz et al., 2006).	29
Figure 2.9	Validation of the simulated left ventricular pressure curves optimized using systolic cuff pressure for the eight human patients with catheter data. Gray lines show cuff measurement systolic and diastolic pressures - only catheter pressure was available as the reference for Patient H.	39
Figure 2.10	Validation of the simulated left ventricular pressure curves for the eight human patients with catheter data after optimizing with measured diastolic cuff pressure as a reference for aortic diastolic pressure. Gray lines show cuff measurement systolic and diastolic pressures - only catheter pressure was available as the reference for Patient H.	40

Figure 3.1	A flowchart of the Design Under Uncertainty (DUU) framework.	45
Figure 3.2	A representative example of a tuned model. (A) Parameterization of an input variable distribution, where $n = 5$. (B) Error fitting of the simulated result with a reference CDF.	47
Figure 3.3	A schematic, showing geometric parameters, and output P-V loop, showing the deterministic metrics, of the CircAdapt model. (A) A schematic of the CircAdapt model highlighting key geometric dimensions of major model components. (B) A typical simulated left ventricular (LV) pressure-volume loop showing both metrics. Pulm. = pulmonary circulation; Syst. = systemic circulation; LA = left atrium; RA = right atrium; RV = right ventricle; EDV = end-diastolic volume.	52
Figure 3.4	Results of Example 1.	54
Figure 3.5	Convergence of resulting input CDFs from Example 1.	55
Figure 3.6	Results of Example 2.	55
Figure 3.7	Convergence of resulting input CDFs from Example 2.	56
Figure 3.8	Results of Example 3.	57
Figure 3.9	Variation of input CDFs from Example 3 with increasing values of N	58
Figure 3.10	Resulting input and output CDFs from a two-dimensional real-world problem, where both probabilistic inputs are tuned and do not have prior-known solutions. The bounds of the plots of x_1 and x_2 represent the bounds of the surrogate.	58

ACKNOWLEDGEMENTS

First, I want to thank my co-advisors, Dr. Adarsh Krishnamurthy and Dr. Baskar Ganapathysubramanian, for their boundless enthusiasm and guidance. I have learned so much from working with them and am fortunate to have had the experiences and conversations we shared, which I will miss dearly.

I am also grateful for the encouragement of the rest of my committee. Particularly, I am indebted to the assistance and support given by Dr. Judy Vance – her advice and judgment helped keep me on track at many crucial periods of my graduate career. Dr. Ming-Chen Hsu played a large role in this work by introducing me to cardiac modeling and teaching me much about the day-to-day process of science. Finally, Dr. James Oliver was a joy to work with and could always offer some insight on the potential application of a new idea.

Many of the graduate students that were my peers at Iowa State University have become good friends. I would specifically like to thank Balaji Sesha Sarath Pokuri, for his expertise and effort pertaining to the surrogate generation, and Austin Herrema, for helping me stay excited during the most difficult parts of the process. Minhua Long, a labmate under my first advisor, was also extremely influential at the start of my PhD.

I especially need to thank my parents and siblings, as well as some extremely close friends, for contributing more than I can possibly hope to list. Without their help, I cannot imagine being prepared for this incredible undertaking.

Lastly, the final stretch of this work is owed in some small part to my dog Leeloo, for her ‘emotional support’ and ‘advice’ during endless nights at the computer when everyone else had long since gone to bed.

ABSTRACT

Patient-specific cardiac models can be used to improve the diagnosis of cardiovascular diseases. However, practical application of these models is impeded by the computational costs and numerical uncertainties of fitting them to clinical measurements from individual patients. Reliable and efficient model tuning within medically-appropriate error bounds is a requirement for practical deployment in the time-constrained environment of the clinic. In this work, we present a framework to efficiently tune parameters of patient-specific mechanistic models using routinely acquired non-invasive patient data with a hybrid particle swarm and pattern search optimization algorithm.

The proposed framework is used to tune full-cycle lumped parameter circulatory models using clinical data obtained from patients as well as canine subjects; showing that the framework can be easily adapted to optimize cross-species models. It is also used to simultaneously obtain the unloaded geometry and passive myocardial material parameters of four left-ventricular cardiac finite element models constructed from canine subject MRI data. This demonstrates that the proposed approach can support the use of complex models to obtain data that cannot be directly measured. The patients gave informed consent and the canine subject studies were approved by the local Institutional Review Boards. The optimized results in all case studies were within acceptable error tolerances.

Additionally, the framework is extended to include uncertainty quantification – supporting model tuning with often-unreliable data sources that are ill-suited to a deterministic approach. The proposed approach for probabilistic model tuning discovers distributions of model inputs which generate target output distributions. Probabilistic sampling is performed using a model surrogate for computational efficiency and a general distribution parameterization is used to describe each input. The approach is tested on four test cases

using CircAdapt, a cardiac circulatory model. Three test cases are synthetic, aiming to match the output distributions generated using known reference input data distributions, while the fourth example uses real-world patient data for the output distributions to obtain the input distribution. The results demonstrate accurate reproduction of the target output distributions, with accurate recreation of reference inputs for the three synthetic examples.

Overall, this work automates the use of biomechanics and circulatory cardiac models in both clinical and research environments by ameliorating the tedious process of manually fitting model parameters and supports the use of more complex models in practice through the quantification of error.

CHAPTER 1. INTRODUCTION

Cardiovascular disease (CVD) has been the leading global cause of death for the last decade, causing roughly a third of total deaths in 2010 ([World Health Organization, 2008](#)). Mortality rates due to CVD have risen owing to lifespan increases in high-income countries ([The World Bank, 2012](#)). The United States, for example, spent an estimated \$193 billion on the treatment of CVD and stroke between 2011 and 2012, more than double the treatment cost of cancer. An additional \$123 billion of future productivity was lost due to premature deaths ([Fuchs and Milstein, 2011](#)).

The cost of treating CVD in the US is significantly higher, for sub-par life expectancy, than other high-income countries ([Mozaffarian et al., 2015](#)). Efforts to improve treatment efficiency, such the American College of Cardiologys Appropriate Use Criteria for cardiovascular technology ([Hendel et al., 2013](#)), are hamstrung by limited adherence to clinical best practices ([Mehta et al., 2007](#)). As an example, only 66.5% of coronary artery disease patients received the optimal evidence-based combination of treatments during their first visit in 2013 ([Maddox et al., 2014](#)). Aside from missed treatment opportunities, these therapies have a large societal cost in the form of adverse drug reactions and unnecessary resource use ([Landrigan et al., 2010](#)). Consistent evaluation of treatment value and risk is necessary to correct these inefficiencies; however, the aggregate value of potential outcomes can be complicated to define or evaluate ([Porter, 2010](#)).

Patient data is widely used to improve risk classification and treatment based on population statistics ([Gaziano et al., 2005](#); [Ferrario et al., 2005](#); [Wilson et al., 1998](#)). While certain acute medical episodes may have clearly preferred treatment strategies, preventa-

tive procedures and the management of chronic illness often involve subjective trade-offs. In these cases, there are often important details in patient data that could impact diagnosis. Unfortunately, declines in cardiac examination skills ([Vukanovic-Criley et al., 2006](#)) and patient-physician interaction time ([Dugdale et al., 1999](#)) have led to a decrease in diagnostic accuracy.

Computer-based decision support systems offer an opportunity for improved treatment efficiency. These technologies are often minimally invasive and make use of commonly recorded medical data to supplement understanding of a patient's condition. Future versions of these models could suggest alternate diagnoses and treatments informed by the rapid developments in machine learning techniques. Physical models have been a foundational category of computer-based medical decision aids for at least 30 years ([Shortliffe et al., 1979](#)), and advances in algorithms and computing power continue to improve the tractability of higher-fidelity analysis ([Baillargeon et al., 2014](#)). However, while computational models can be used to more efficiently and thoroughly understand a complex system than experiments at a reduced cost, many components require manual or automated tuning of model parameters to properly capture the modeled system.

The deployment of more complex models is currently limited by the expensive tuning of many patient-specific parameters and the level of training required to initialize and operate them. Additionally, the values of these parameters are often determined using experimental or reference data, either directly or indirectly via dependent model values. Available data is often unreliable which impedes consistent tuning and must be accounted for to fully determine the accuracy of a result.

I propose an optimization-based framework to support the wider application of patient-specific physical models to the treatment of CVD. Optimization provides a useful framework to bridge the gap between available models and patient data by automating the parameter selection process. The main contributions of this dissertation include the development of:

1. **A framework to automatically tune biomechanics and circulatory cardiac models using patient-specific data**

Cardiovascular applications of optimization have focused on shape optimization of cardiac geometry using idealized template meshes. Recently, biomechanics and circulatory models have increased in complexity, allowing them to capture the physics more accurately. However, improvements in optimization methodologies have not been widely applied specifically to parameter estimation of these physics models. [Marsden et al. \(2008\)](#) used the surrogate management framework (SMF) for shape optimization with a general biophysical model. [Agoshkov et al. \(2006\)](#) used an adjoint approach to geometrically optimize an idealized model of cardiac anastomosis. [Krishnamurthy et al. \(2013\)](#) hand-tuned a model of ventricular inflation with patient-specific geometry to determine cardiac tissue material parameter inputs of a circulatory model. I created an optimization framework to tune the parameters of biomechanics and circulatory cardiac models based on patient-specific data, allowing physicians to more broadly apply these models in a clinical setting.

2. **A reliable optimization formulation to fit parameters of full cardiac-cycle circulatory models**

Most previous applications of optimization to circulatory model parameter fitting have used a localized or gradient-based approach; however, derivative-free and heuristic methods are more suitable for complex, multimodal models. [Neal and Bassingthwaite \(2007\)](#) used the Nelder-Mead Simplex algorithm (NMS) to tune two open-loop models of hemorrhage in porcine subjects. [Lim et al. \(2010\)](#) applied NMS to explore a lumped parameter model of an implantable rotary blood pump under various operating conditions. [Ellwein et al. \(2013\)](#) used the gradient-based LevenbergMarquardt algorithm to fit a lumped-parameter model of congestive heart failure. I demonstrate an efficient and reliable algorithm for optimizing full-cycle circulatory models that can work for a wide variety of patients.

3. **A methodology suitable for treatment and study utilizing cross-species models**

Medical scientists commonly use animals to perform research more feasibly than could be done with human patients (Leong et al., 2015). Different animal models are valued for the study of specific aspects of cardiac function (Milani-Nejad and Janssen, 2014), necessitating the development of consistent study methodologies to compare results. Most cross-species research has focused on the study of drug response in living subjects; computerized biophysical models are a less mature field and are thus still establishing best practices. I show that the proposed framework can be used to consistently analyze models of both human patients and canine subjects, validating its suitability for cross-species research.

4. **A platform for uncertainty quantification (UQ) of patient-specific biophysical models**

Physicians cannot rely on models unless the error of a simulated result is quantified. Analysis of parameter sensitivity can be used to obtain this information or provide a more robust solution. These techniques are mature, but have not been widely applied to patient-specific models. Sankaran et al. (2013) modeled the long-term adaptation of blood vessels by robustly optimizing arterial wall properties of an idealized geometry using SMF with a stochastic cost function. Probst et al. (2010) studied the sensitivity of idealized bypass geometry to blood viscosity inputs by computing derivatives of geometric parameters. Huberts et al. (2018) propose a method to make uncertain cardiovascular models more useful for diagnosis and intervention based largely on sensitivity analysis. Sankaran and Marsden (2011) perform UQ for a variety of geometric cardiovascular models using a stochastic collocation approach. I describe and test an appropriate method of UQ for patient-specific biophysical models as a foundational step towards quantifying the confidence in their results.

This work facilitates the use of biomechanics and circulatory cardiac models by addressing the currently most challenging aspects of the process. Researchers will also be able to build on this framework to compare data between cross-species models and further advance medical understanding. Chapter 2 introduces the deterministic portion of the framework. In Chapter 3, it is extended to include uncertainty quantification. Finally, Chapter 4 summarizes results and limitations and highlights potential avenues of improvement.

CHAPTER 2. OPTIMIZATION FRAMEWORK FOR PATIENT-SPECIFIC CARDIAC MODELING

This paper is in review for *Biomechanics and Modeling in Mechanobiology*. It was authored by Joshua Mineroff, Andrew D. McCulloch, David Krummen, Baskar Ganapathysubramanian, Adarsh Krishnamurthy. I was responsible for developing, implementing, and testing the framework as well as for writing the majority of the manuscript. Andrew and David offered expertise on cardiovascular disease and treatment. Baskar contributed to the methodological decisions pertaining to optimization. Adarsh helped create the methodology and informed relevance to the field of cardiac modeling.

2.1 Abstract

Patient-specific models of the heart can be used to improve the diagnosis of cardiac diseases, but practical application of these models can be impeded by the computational costs and numerical uncertainties of fitting mechanistic models to clinical measurements from individual patients. Reliable and efficient tuning of these models within clinically appropriate error bounds is a requirement for practical deployment in the time-constrained environment of the clinic. We developed an optimization framework to efficiently tune parameters of patient-specific mechanistic models using routinely-acquired non-invasive patient data. We employ a hybrid particle swarm and pattern search optimization algorithm, but the framework can be readily adapted to use other optimization algorithms. We apply the proposed framework to tune full-cycle lumped parameter circulatory models using clinical data obtained from patients who gave informed consent. We show that our framework

can be easily adapted to optimize cross-species models by tuning the parameters of the same circulation model to four canine subjects. Finally, to demonstrate the framework's extensibility to more sophisticated models, we use it to simultaneously obtain the unloaded geometry and optimize the passive myocardial material parameters of four left-ventricular cardiac finite element models constructed from canine subject MRI data. The simulated end-diastolic pressure-volume relationships were optimized to match previously established relationships from literature (Klotz *et al.*, 2006); and were all within acceptable error tolerances. This work will facilitate the use of biomechanics and circulatory cardiac models in both clinical and research environments by ameliorating the tedious process of manually fitting the parameters.

2.2 Acknowledgements

This research was supported in part by the National Biomedical Computation Resource, NIH Grant 8 P41 GM103426-21 (Amaro and McCulloch), by the UC Center for Accelerated Innovation under NIH grant 4 U54 HL11-9893, NIH grant 1 R01 HL131753 (Segars, Krishnamurthy, McCulloch), by NSF grant 1750865 (Krishnamurthy), and by the Joseph C. and Elizabeth A. Anderlik Professorship at Iowa State University (Mineroff). We would also like to show our gratitude to Dr. Judy Vance at Iowa State University for her extraordinary support.

ADM is a co-founder, equity holders and scientific advisory board member of Insilicomed Inc. and Vektor Medical, licensees of UCSD software used in this research. This relationship has been disclosed to the University of California San Diego and is overseen by an independent conflict of interest management subcommittee appointed by the university. The other authors have declared that no competing interests exist.

2.3 Introduction

Cardiovascular disease (CVD) has been the leading cause of death globally for the last decade, causing roughly a third of all-cause deaths in 2013 (Roth et al., 2015). Efforts to improve treatment efficiency, e.g. the development of appropriate use criteria for cardiovascular technology (Hendel et al., 2013), have been hamstrung by limited adherence to clinical best practices (Mehta et al., 2007) mainly due to the complicated nature of CVD, declines in cardiac examination skills (Vukanovic-Criley et al., 2006), and reduced patient-physician interaction time (Dugdale et al., 1999). As an example, only 66.5% of coronary artery disease patients received the optimal evidence-based combination of treatments during their first visit in 2013 (Maddox et al., 2014). Suboptimal initial treatment increases effective time-to-treatment, further contributing to CVD mortality rates (Nallamotheu et al., 2015; Ting et al., 2010). Patient-specific computer-based decision support systems offer an opportunity for improved treatment efficiency through better diagnosis based on mechanistic models tuned to the individual patient.

Physical models have been a foundational category of computer-based medical decision aids for at least 30 years (Shortliffe et al., 1979) and advances in algorithms and computing power continue to improve the tractability of higher-fidelity analysis (Baillargeon et al., 2014). Specifically, patient-specific computer-based decision support systems often make use of commonly recorded medical data to assist clinical diagnosis or therapy planning. Graphical decision aids have also been found to improve comprehension when used to supplement physician-patient discussions (Stacey et al., 2017; Hess et al., 2012; Arnold et al., 2008). As an example, cardiac pressure-volume (P-V) loops are an effective tool for the identification of cardiac pathologies, since cardiologists are trained to diagnose different pathological conditions using them. P-V loops of the ventricular chambers are traditionally unobtainable without catheterization, but computational mechanistic models can estimate P-V loops of each chamber of the heart using only non-invasive measurements.

Patient data is widely used for risk classification and forecasting of treatment outcomes based on population statistics (Gaziano et al., 2005; Ferrario et al., 2005; Wilson et al., 1998); patient-specific modeling is the process of using these data to individualize general computational models to integrate clinical data and use prior physiological knowledge and physicochemical constraints to make individualized predictions and decisions. However, the deployment of complex patient-specific models is currently limited by the level of training required to initialize and operate them. Individualizing a complex model for a wide variety of patients is often hindered by gaps in available patient data, which necessitate the use of empirical data or rules to tune model parameters. Reliable and efficient tuning of these models is a requirement for deployment in the environment of a medical clinic, but the manual tuning process can be imprecise and time-consuming.

In order to reduce the manual tuning required for patient-specific modeling, we propose an optimization-based framework to support the wider application of patient-specific physical models to the treatment of CVD. Optimization bridges the gap between available complex models and patient data by automating the fitting process and providing a consistent, resource-efficient result. Manual tuning relies heavily on the user’s experience with the model, and modeled system, to select appropriate parameters; this often leads to local optima that are unnecessarily close to initially-assumed parameter values. Computerized optimization can systematically search the feasible region more efficiently, often running many evaluations in parallel, to find better solutions.

We test this framework using two examples: a left ventricular (LV) passive finite-element model and a hemodynamic lumped-parameter circulation model. The FEA model is used to determine the unloaded geometry and the cardiac tissue material parameters of four canine subjects based on data made available from a previous benchmark study (Wang et al., 2009). The circulation model is then used to personalize the hemodynamics of the four canine subjects to generate P-V loops of the different chambers of the heart. The framework is then used to determine the hemodynamic parameters of eight human patients

using only limited non-invasive measurements. This demonstrates the broad applicability of the proposed method in handling different mechanistic models in different species.

The main contributions of this work include the development of:

1. A framework to automatically tune biomechanics and circulatory cardiac models using patient-specific data with minimal user intervention.
2. A robust optimization formulation to fit parameters of full cardiac-cycle circulatory models, even with missing clinical data in certain patients.
3. A methodology that is applicable for different types of mechanistic models and enable automatic tuning of cross-species models.

Our optimization framework can be used by researchers who can treat the mechanistic models as a black-box. It will facilitate the use of biomechanics and circulatory cardiac models in both clinical and research environments by ameliorating the tedious and potentially biased process of manually fitting the parameters.

2.4 Related Work

Recently, cardiovascular models have increased in complexity, allowing them to capture the relevant physics more accurately. Highly sophisticated models exist for many biophysical cardiac phenomena, (Niederer et al., 2009) and treatment options (Kerckhoffs et al., 2008). These models require extensive patient data and are already being tested in clinical settings. Smith et al. (2011) are developing one such example of a data driven-model for the optimal application of treatment modalities.

Cardiovascular applications of optimization to biomechanics and circulatory models have focused on shape optimization of cardiac geometry using idealized template meshes. However, improvements in optimization methodologies have not been widely applied specifically to parameter estimation of these physics models. Marsden et al. (2008) used the surrogate management framework (SMF) for shape optimization with a general biophysical model.

[Agoshkov et al. \(2006\)](#) used an adjoint approach to geometrically optimize an idealized model of cardiac anastomosis. [Krishnamurthy et al. \(2013\)](#) hand-tuned a model of ventricular inflation with patient-specific geometry to determine cardiac tissue material parameter inputs of a circulatory model.

Closed-loop circulatory models provide valuable insight into cardiac function. Early circulatory models were limited to small sections of the cardiovascular system ([Hardy et al., 1982](#)), but increases in computing power enabled the development of more complete models. For example, [Olansen et al. \(2000\)](#) constructed an integrative model using reference values to study the effects of small parameter perturbations. This model, and others like it, were primarily valuable as a tool to develop and test general physiological principles. The CircAdapt model consists of an idealized set of active components (i.e. tubes, chambers, and valves) that are governed by empirical and patient-specific data ([Arts et al., 2005](#)).

Most previous applications of optimization to circulatory model parameter fitting have used a localized or gradient-based approach; however, derivative-free and heuristic methods are more suitable for complex, multi-modal models where gradient-evaluation is expensive and there are many local optima that confuse the solver. [Neal and Bassingthwaight \(2007\)](#) used the Nelder-Mead Simplex algorithm (NMS) to tune two open-loop models of hemorrhage in porcine subjects. [Lim et al. \(2010\)](#) applied NMS to explore a lumped parameter model of an implantable rotary blood pump under various operating conditions. [Ellwein et al. \(2013\)](#) used the gradient-based Levenberg-Marquardt algorithm to fit a lumped-parameter model of congestive heart failure.

Medical science commonly uses animals to perform research more feasibly than could be done with human patients ([Leong et al., 2015](#)). Different animal models are valued for the study of specific aspects of cardiac function ([Milani-Nejad and Janssen, 2014](#)), necessitating the development of consistent study methodologies to compare results. Most cross-species research has focused on the study of drug response in living subjects; computerized biophysical models are a less mature field and are thus still establishing best practices.

We created an optimization framework to tune the parameters of biomechanics and circulatory cardiac models generated using patient-specific data, allowing physicians to more broadly apply these models in a clinical setting. The burden of parameter tuning is reduced by using adaptation rules to propagate changes through the model, making CircAdapt ([Arts et al., 2005](#)) an especially tractable patient-specific model. We demonstrate an efficient and reliable algorithm for optimizing full-cycle circulatory models and show that the proposed framework can be used to consistently analyze models of both human patients and canine subjects, validating its suitability for cross-species research.

2.5 Methods

2.5.1 Optimization framework

Our framework is designed to perform parameter optimization to tune patient-specific computerized biophysical models to available data. The multi-modal, highly corrugated nature of these models makes it difficult to compute gradients and favored a derivative-free approach. We selected a hybrid particle swarm and pattern search solver to globally search the parameter space and support parallel model evaluation. Since model analysis is the primary computational expense for this class of problems, the potential overhead of a higher-level software package is insignificant.

Particle swarm optimization (PSO) is a heuristic method using a population of candidate solutions, referred to as particles ([Shi and Eberhart, 1998](#)). Initially, these particles are distributed throughout the parameter space with a given location and 'velocity.' A step of the algorithm starts with the evaluation of the current parametric configuration of each particle. Then, the velocities of each particle are updated as a function of (1) its current velocity, (2) the best solution that it has found, and (3) the best solution any particle has found. The algorithm continues until a termination criteria is met, usually when a set number of iterations have passed without improving the objective value by a given tolerance.

One of the primary benefits of PSO is its fast convergence in global search for traditionally difficult problems, but it is an expensive method for computing precise optima.

Pattern search is a direct search method (DS) involving the use of a scalable pattern, or mesh, to step through the parameter space from an initial location ([Hooke and Jeeves, 1961](#)). At each iteration, the mesh is centered at the current best point and parameter values at the surrounding mesh points are evaluated. The specific mesh pattern used polls a positive and negative perturbation of every parameter at each iteration. If an improvement is found, the mesh is re-centered at the new location and expanded to minimize the chances of convergence to a non-global minimum. If no improvement is found, the mesh is contracted to more precisely identify the local optimum. DS methods are highly influenced by initially assumed parameter values, but are one of the most efficient non-analytical methods for the identification of a precise solution.

The full hybrid algorithm we employed first searches the solution space using PSO to identify a likely global optima. The resulting solution was then used to initialize the DS method to more efficiently find a precise optimum. It is generally impossible to prove that the true global optimum has been identified for non-analytical multi-modal problems, but in our experience, this approach converged to an acceptable result within the bounded parameter space for a majority of the runs.

All optimization and analysis was run on a cluster with each node having two 2.6 GHz 8-Core Intel E5-2640 v3 processors and 128GB of RAM. The framework is implemented in MATLAB ([MathWorks, 2017](#)), since it has multiple commercially-tested derivative-free solvers and is capable of integrating with most models, and will be made available after publication. The primary computational expense for the kind of optimization problems studied in this paper are the many model evaluations required. Both optimization methods used in our approach are well-suited to parallelization which can decrease the wall time of the optimization by allowing a larger pool of computational resources to be used than could be applied to a single evaluation. This is especially attractive with the increasing use

of cloud computing. Parallelization was handled differently for each model and is further explained in each section.

2.5.2 Clinical data

The eight human patients studied were male, aged (66 ± 11 years) with NYHA class III heart failure, dilated cardiomyopathy, and left bundle branch block (LBBB) were enrolled from the Veteran’s Administration San Diego Healthcare System (San Diego, CA). Patients gave informed consent to participate in the human subject protocol approved by the institutional review board. Key cardiac measurements were recorded via echocardiogram and routine diagnostic methods; pressure data from cardiac catheterization was also used for validation.

The canine simulations used four normal dog data provided by the STACOM 2014 LV Mechanics Challenge ([Camara et al., 2014](#)). The data was acquired at the National Institute of Health, USA in collaboration with Johns Hopkins University ([Ennis, 2004](#)) using high resolution cines, tagging, and ex-vivo diffusion tensor imaging (DTI) ([Wang et al., 2009](#)). Data acquisition was approved by local Institutional Review Boards and conducted in accordance with the “Guide for the Care and Use of Laboratory Animals” ([Institute of Laboratory Animal Resources \(ILAR\), 1996](#)). In-vivo left ventricular pressures were also recorded during scanning. Dogs were paced from the right atrium. The processed data included mesh point clouds and binary masks defining the LV geometry and muscle fiber orientations derived from ex vivo diffusion tensor MRI. The geometries only reflect the location of the epicardial and endocardial surfaces; they do not encode material point displacements. The finite element geometry for the dog models were reconstructed using the methods outlined in [Krishnamurthy et al. \(2015\)](#).

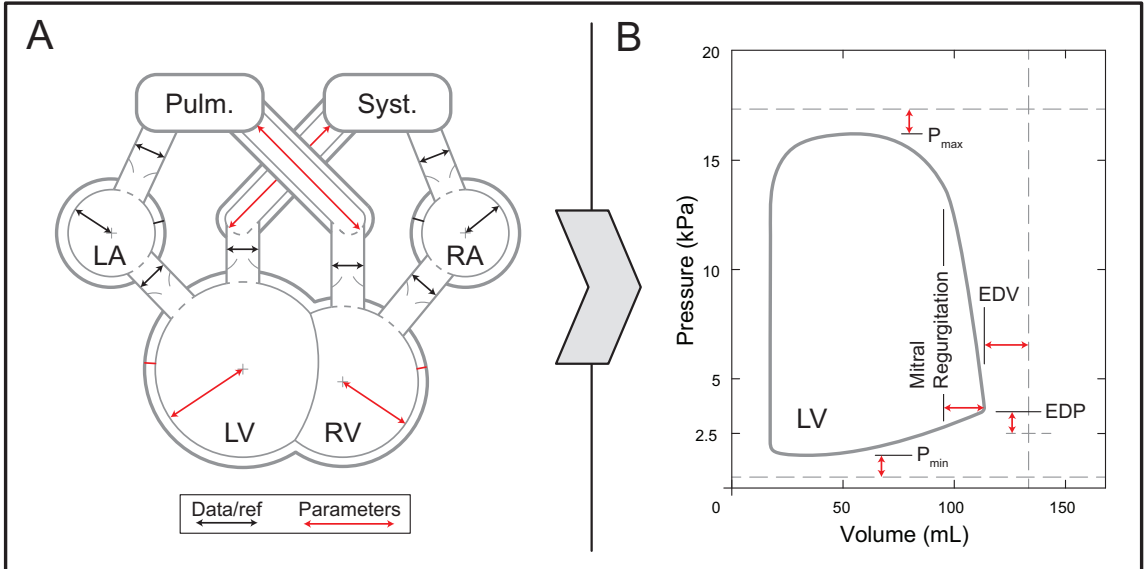


Figure 2.1 The geometric parameters and objective metrics used in the circulatory optimization. (A) A schematic of the CircAdapt model highlighting key geometric dimensions of major model components. A subset of the model values directly driven by patient-specific or reference data (Table 2.1) and the parameters used (Table 2.3) are both shown. (B) A typical simulated left ventricular (LV) pressure-volume loop showing all partial objective metrics. Pulm. = pulmonary circulation; Syst. = systemic circulation; LA = left atrium; RA = right atrium; RV = right ventricle; EDV = end-diastolic volume; EDP = end-diastolic pressure.

2.5.3 Circulation model

CircAdapt (Arts et al., 2005) is a lumped-parameter model of the circulatory system (Fig. 2.1) implemented in MATLAB. It can be used to model the pressure and volume of the four chambers as a function of time for the complete cardiac cycle. We use CircAdapt to perform a closed-loop simulation of the patient-specific cardiovascular system, incorporating up to 11 values of non-invasively obtained patient data, and output one simulated cycle of blood flow. The potential data include heart rate and blood pressure, as well as valve measurements that can be obtained through ECG or echocardiogram (Table 2.1). Basic canine subject data was also used (Table 2.2). A subset of seven CircAdapt model parameters were selected for tuning (Table 2.3).

Table 2.1 Experimentally measured and reference data for human patients studied in circulatory optimization. Missing measurements were substituted with appropriately scaled reference values. HR = heart rate; q = mean systemic blood flow; QRS = QRS complex duration; D_{aorta} = diameter of aorta; D_{aortic} = diameter of aortic valve; D_{pulm} = diameter of pulmonary artery; D_{mitral} = diameter of mitral valve; V_{wall} = ventricular wall volume; P_{maxLV} = peak left-ventricular pressure; EDV_{LV} = left-ventricular end-diastolic volume; MRV = mitral regurgitant volume.

Patient	HR (BPM)	q (mL/s)	QRS (s)	D_{aorta} (m)	D_{aortic} (m)	D_{pulm} (m)	D_{mitral} (m)	V_{wall} (m ³)	P_{maxLV} (kPa)	EDV_{LV} (mL)	MRV (mL)
<i>ref</i>	71	$85e-6$	-	$25e-3$	$25e-3$	$26e-3$	$25e-3$	$213e-6$	16.3	118	-
A	70	$80e-6$	0.156	$22e-3$	$34e-3$	-	$18e-3$	$260e-6$	18.7	235	-
B	70	$51e-6$	0.148	$34e-3$	$18e-3$	-	$16e-3$	$190e-6$	14.7	177	15
C	70	$100e-6$	0.162	-	$22e-3$	$18e-3$	$23e-3$	$270e-6$	15.5	142	-
D	70	$84e-6$	0.130	-	$24e-3$	$15e-3$	$23e-3$	$450e-6$	20.1	289	30
E	60	$45e-6$	0.128	-	$22e-3$	-	$42e-3$	$450e-6$	13.1	257	5
F	70	$55e-6$	0.119	$25e-3$	$25e-3$	-	$25e-3$	$309e-6$	9.5	135	-
G	70	$46e-6$	0.140	$36e-3$	$23e-3$	-	$16e-3$	$290e-6$	6.7	198	-
H	70	$56e-6$	0.124	$35e-3$	$21e-3$	-	$16e-3$	$237e-6$	16.3	166	-

Table 2.2 Experimentally measured objectives for canine subjects studied in circulatory optimization. All subject models relied largely on reference data. $Pmax_{LV}$ = peak left-ventricular pressure; EDV_{LV} = left-ventricular end-diastolic volume.

Subject	$Pmax_{LV}$ (kPa)	EDV_{LV} (mL)
S1	13.6	30.3
S2	12.3	20.5
S3	10.3	24.5
S4	11.3	19.6

Primary model fit was assessed as a function of the relationships of simulated peak pressure ($Pmax$, Eq. 2.1) and end-diastolic volume (EDV , Eq. 2.2) to measured patient values, with additional constraints that are enforced as penalties to the objective function. These penalties were based on (1) minimum LV pressure ($Pmin$: 0.5 kPa, Eq. 2.3), (2) LV end-diastolic pressure (EDP : 2.5-4 kPa, Eq. 2.4), and (3) mitral regurgitant volume (MRV , Eq. 2.5). The component weights of the objective function were selected to prioritize those with greater certainty and reduce those relying on assumptions from reference data. The contribution of constraints on $Pmin$ and EDP were minimized the most, as they were not derived from patient data, while $Pmax$ was weighted highly, as it was measured most directly. Additionally, positive $Pmax$ and EDV model error were penalized by a factor of 2 to account for possible measurement overestimation (Piper et al., 2015; Lang et al., 2006). If no MRV patient data was available, then a healthy reference value of 30 mL was used as an upper bound; 3 mL was used for the canine subjects. Our framework could be easily adapted to use other objective functions motivated by biomechanical principles or physiology (e.g. Heusinkveld et al. (2009)).

Table 2.3 Parameters and bounds of the different optimization variables in \mathbf{x} of the circulation model.

Variable	Description	Lower Bound	Upper Bound	Units	Reference
k_{MAP}	Scaling of mean arterial pressure initially calculated using the '33% formula'	0.8	1.2	-	(Raamat et al., 2013)
$P\Delta_{pulm}$	Blood pressure head loss across the pulmonary system	0.5	1.5	kPa	(Yoshimura et al., 1993; Nauser and Stites, 2001)
L_{aorta}	Geometric scaling factor of effective length of aorta from CircAdapt reference configuration	0.5	1.5	-	
L_{pulm}	Geometric scaling factor of effective length of pulmonary artery from CircAdapt reference configuration	0.5	1.5	-	
k_{LV}	Geometric scaling factor of left ventricular midwall surface area from CircAdapt reference configuration	0.5	2	-	(Clay et al., 2006)
k_{RVrel}	Geometric scaling factor of right ventricular midwall surface area from CircAdapt reference configuration relative to left ventricle scaling	0.5	2	-	(Kovalova et al., 2006)
Sf_{act}	Maximum isometric active stress of myofibers	25	200	kPa	
Sf_{pas}	Passive stiffness of myofibers	10	30	kPa	
M_{leak}	Ratio of mitral valve leak area to open area	1e-6	0.2	-	(Zoghbi, 2016)

$$y_{Pmax}(\mathbf{x}) = \begin{cases} \left(\frac{Pmax(\mathbf{x}) - Pmax_{data}}{Pmax_{data}} \right)^2, & \text{if } Pmax(\mathbf{x}) \leq Pmax_{data} \\ 2 * \left(\frac{Pmax(\mathbf{x}) - Pmax_{data}}{Pmax_{data}} \right)^2, & \text{if } Pmax(\mathbf{x}) > Pmax_{data} \end{cases} \quad (2.1)$$

$$y_{EDV}(\mathbf{x}) = \begin{cases} \left(\frac{EDV(\mathbf{x}) - EDV_{data}}{EDV_{data}} \right)^2, & \text{if } EDV(\mathbf{x}) \leq EDV_{data} \\ 2 * \left(\frac{EDV(\mathbf{x}) - EDV_{data}}{EDV_{data}} \right)^2, & \text{if } EDV(\mathbf{x}) > EDV_{data} \end{cases} \quad (2.2)$$

$$g_{Pmin}(\mathbf{x}) = \left(\frac{Pmin(\mathbf{x}) - Pmin_{ref}}{Pmax_{data} - Pmin_{ref}} \right)^2, \quad \text{if } Pmin(\mathbf{x}) > Pmin_{ref} \quad (2.3)$$

$$g_{EDP}(\mathbf{x}) = \begin{cases} \left(\frac{EDP(\mathbf{x}) - EDP_{refmin}}{Pmax_{data} - Pmin_{ref}} \right)^2, & \text{if } EDP(\mathbf{x}) \leq EDP_{refmin} \\ \left(\frac{EDP(\mathbf{x}) - EDP_{refmax}}{Pmax_{data} - Pmin_{ref}} \right)^2, & \text{if } EDP(\mathbf{x}) > EDP_{refmax} \end{cases} \quad (2.4)$$

$$g_{MRV}(\mathbf{x}) = \begin{cases} \left(\frac{MRV(\mathbf{x}) - MRV_{data}}{MR_{data}} \right)^2, & \text{if } MRV_{data} \neq \emptyset \\ \left(\frac{MRV(\mathbf{x}) - MRV_{ref}}{MR_{ref}} \right)^2, & \text{if } MRV_{data} = \emptyset \\ & \text{and } MRV(\mathbf{x}) > MRV_{ref} \end{cases} \quad (2.5)$$

The complete optimization formulation (Eq. 2.6) was used to generate CircAdapt models for eight human patients and four canine subjects. This resulted in 45 (5N) evaluations for

each PSO iteration and 18 (2N) iterations for each DS iteration. Each optimization was run in a MATLAB environment on one 16-core node, allowing for 16 parallel single-threaded evaluations. Repeated parameter configurations used the initial result for improved efficiency.

$$\begin{aligned}
& \arg \min_{\mathbf{x}} \left(0.8 * y_{Pmax}(\mathbf{x}) + 0.2 * y_{EDV}(\mathbf{x}) \right. \\
& \quad \left. + 0.75 * g_{Pmin}(\mathbf{x}) + 0.75 * g_{EDP}(\mathbf{x}) \right. \\
& \quad \left. + 0.15 * g_{MRV}(\mathbf{x}) \right) \tag{2.6} \\
& \text{s.t.} \quad E(P(\mathbf{x}), V(\mathbf{x})) = 0, \quad (\text{ODE Solution}), \\
& \quad \quad \quad A\mathbf{x} \leq b, \quad (\text{Bounds on } \mathbf{x})
\end{aligned}$$

2.5.4 Finite-element model

We use a finite-element model of the canine left ventricle to determine its unloaded state and personalized material parameters of the cardiac tissue. An analysis-suitable left ventricular mesh is constructed from an MRI scan of the subject or patient heart at end-diastole. However, since this mesh is measured at the loaded state, an unloaded mesh state needs to be determined along with the properties of the passive Ogden-Holzapfel material model ([Holzapfel and Ogden, 2009](#)).

The unloaded mesh is obtained through an iterative inflation-deflation process. We first assume an initial unloaded geometry state that is identical to the MRI mesh, and passively inflate it to the measured EDP. Then the deformation gradient between the loaded and MRI mesh is inversely applied to the unloaded geometry. This process is repeated until the interior volume of the loaded mesh and MRI mesh converge to within 3% ([Krishnamurthy et al., 2016](#)).

$$\psi = \frac{a}{2b} e^{b(I_1-3)} + \sum_{i=f,s} \frac{a_i}{2b_i} (e^{b_i(I_{4i}-1)} - 1) + \frac{a_{fs}}{2b_{fs}} (e^{b_{fs}I_{8fs}^2} - 1) \tag{2.7}$$

Table 2.4 Parameters and bounds of coefficients of \mathbf{x} in Eq. 2.9

	a (kPa)	a_f (kPa)	b -	b_f -
Upper Bound	50	50	50	50
Reference	1.5	15	8	15
Lower Bound	0.01	0.01	0.01	0.01

Four material model parameters (a , b , a_f , and b_f , Table 2.4) are used to represent patient-specific material properties in a simplified form of the Ogden-Holzapfel strain energy function (Eq. 2.7). Correctness of the material parameters is determined by the conformation of the resulting inflated ventricle to the reference end-diastolic pressure-volume relationship (EPDVR) described by Klotz et al. (2006). This method uses the sole original end-diastolic pressure (EDP) and volume (EDV) data point to describe the entire EDPVR as a function (Eq. 2.8) with patient-specific values α and β . The least squares error is then calculated between this curve and the complete set of data captured during the simulated inflation (Fig. 2.2). The optimized material parameter values are those that minimize this error (Eq. 2.9). We used four meshes generated from canine subjects to demonstrate the approach.

$$EDP_i = \alpha * EDV_i^\beta \quad (2.8)$$

$$\begin{aligned} \arg \min_x & \sum_{i=1}^n (P_i(x) - \alpha(x)EDV_i(x)^{\beta(x)})^2 \\ \text{s.t.} & E(V(x)) = 0, \quad (\text{PDE Solution}), \\ & Ax \leq b, \quad (\text{Bounds on } x) \end{aligned} \quad (2.9)$$

Evaluation of this model is significantly more expensive than the circulation model, and is therefore optimized using only the more computationally efficient DS portion of the optimization framework. This shows how the exact implementation of the framework can be easily adapted to different problems. The MATLAB-based DS optimization framework

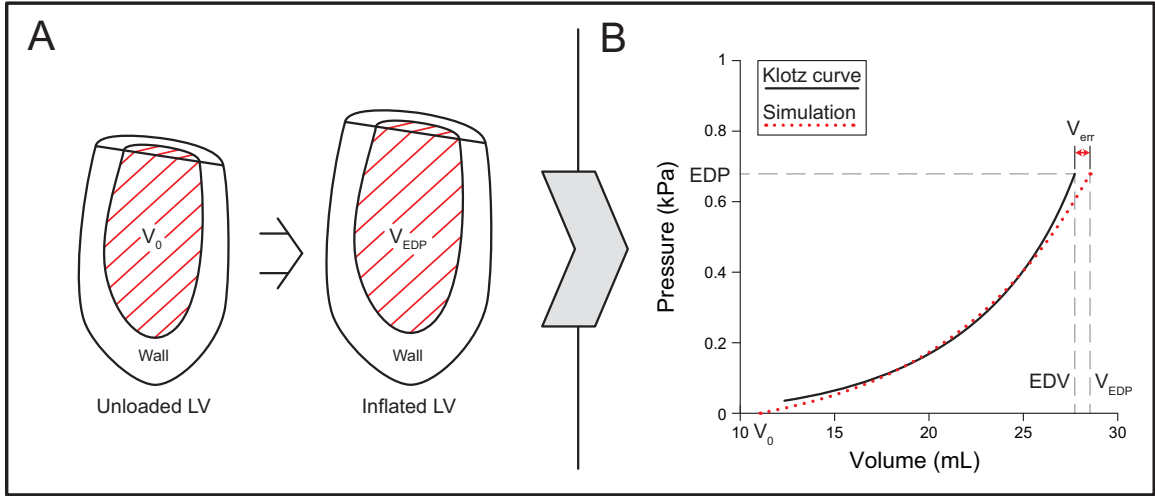


Figure 2.2 A representative example of both mesh states of the finite-element optimization and the resulting EDPVR curve. (A) A converged unloaded and inflated mesh from the simulation showing the change in ventricular shape and volume. (B) A comparison of the precomputed Klotz curve and simulated pressure-volume curve. EDPVR = end-diastolic pressure-volume relationship.

generated eight ($2N$) parameter configurations for each mesh iteration of the optimization algorithm. The evaluation of these was handled via a queue managed by GNU Parallel (Tange, 2011) to run up to eight evaluations in parallel across four nodes. A bash script was used to control the inflation/deflation cycle until the model had converged. Each simulation was performed using Continuity 6.4 (CMRG, 2015), a Python-based multi-scale FEA and modeling tool developed by the UCSD Cardiac Mechanics Research Group, in parallel across eight cores. This approach is highly scalable with a minimal amount of overhead.

2.6 Results

2.6.1 Circulation model results

Patient-specific circulatory models were tuned for the eight human subjects using CircAdapt with the presented optimization framework to determine parameter values (Table 2.5). The pressure error for the eight patients had a max of 0.53% and a mean of 0.15%.

Volume error had a max of 6.71% and a mean of 1.26%. Only the models for patients A and E exceeded the reference minimum pressure value of 1 kPa, with patient E having the highest value of 1.18 kPa, but all models had acceptable EDP values within 18% of the 2.5 kPa reference value. Mitral regurgitant volume was within 1.3 mL of the measured value for two of the patients where that data was available (B and D), and within the (< 30 mL) healthy range for patients that did not have that data. The low measured regurgitant volume (5 mL) of patient E was not able to be satisfied, contributing significantly (30%) to the objective value.

The tuned models for patients A and E had significantly higher optimized objective values than the other six patients ($0.21e-3$ and $1.23e-3$ respectively, compared to the overall median of $6.4e-8$), primarily from EDV error. The model for patient F was the best optimization result, with an objective value of $6e-9$. Parameter values were not consistently bounded and were typically distributed through the allowable range. None of the left ventricular P-V loops from each of the tuned models (Fig. 2.3) have any obvious artifacts that would signify errors in CircAdapt model convergence.

CircAdapt models were also tuned for four canine subjects (Table 2.5), generating a set of P-V loops (Fig. 2.4). The objective values for these models were higher on average than the human patients ($1.95e-3$ vs. $1.8e-4$). The primary source of errors varied across subjects, with S1 being most affected by Pmax and S3 being most affected by EDP and Pmin.

The average time to solution was 29 hrs, with a range of 25-40 hrs. The average number of model evaluations was 3875, ranging from 2257 to 5454; 8% of these were repeat configurations which used the previously logged result for efficiency.

Both sets of circulatory results were validated by calculating the root-mean-square error (RMSE) between the simulated pressure curves and the left ventricular catheter data that was available for the eight patients. The result highlights a potential downside of only using non-invasive measurements, because systolic cuff pressure data for the studied patients

Table 2.5 Optimized parameters and results of human patients and canine subjects studied in circulatory optimization. Bounded optimal parameter values are bolded. Explanation of variables can be found in Table 2.3.

Pat/ Sub	k_{MAP}	$P\Delta_{pulm}$ (kPa)	L_{aorta}	L_{pulm}	k_{LV}	k_{RVrel}	Sf_{act} (kPa)	Sf_{pas} (kPa)	M_{teak}	Obj 1e-3	P_{maxerr} %	EDV_{err} %
<i>ref</i>	1	1.5	1	1	1	1	120	4.0	1e-6	-	-	-
A	1.15	0.50	1.31	0.86	1.57	0.50	200	10.0	7.1e-2	0.21	-0.53	-2.39
B	1.04	0.77	0.68	1.23	1.30	0.53	142	22.9	4.7e-2	0.00	-0.02	-0.00
C	1.18	1.24	1.46	0.54	1.19	0.79	171	24.4	4.5e-3	0.00	0.01	0.00
D	1.15	0.50	1.49	1.46	1.68	0.50	198	10.0	4.7e-2	0.02	-0.03	-0.95
E	0.99	0.50	1.26	0.51	1.48	0.70	158	22.2	8.7e-4	1.23	-0.50	-6.71
F	0.92	0.81	1.00	1.35	1.33	0.63	200	19.4	2.2e-2	0.00	-0.01	-0.01
G	1.04	1.14	0.53	0.64	1.55	0.64	149	24.7	5.4e-2	0.00	0.02	0.00
H	0.95	1.22	1.30	0.91	1.29	1.08	193	29.3	2.9e-2	0.00	-0.03	0.00
μ	1.05	0.84	1.13	0.94	1.42	0.67	176	20.3	0.03	0.18	0.15	1.26
σ	± 0.10	± 0.33	± 0.36	± 0.37	± 0.17	± 0.19	± 24	± 7.0	± 0.02	± 0.43	± 0.23	± 2.36
S1	1.06	1.50	0.92	0.53	1.28	1.30	194	10.1	1e-6	0.22	-0.45	0.05
S2	1.06	1.30	1.48	1.49	1.18	0.53	171	10	1.3e-6	0.10	-0.14	-0.33
S3	1.13	1.42	1.25	1.29	1.28	0.53	153	28.7	1.3e-3	7.48	0.02	-0.27
S4	1.11	1.03	0.50	1.50	1.17	0.71	115	29.7	1e-6	0.00	0.14	-0.08
μ	1.05	0.84	1.13	0.94	1.42	0.67	176	20.3	0.03	0.18	0.15	1.26
σ	± 0.10	± 0.33	± 0.36	± 0.37	± 0.17	± 0.19	± 24	± 7.0	± 0.02	± 0.43	± 0.23	± 2.36

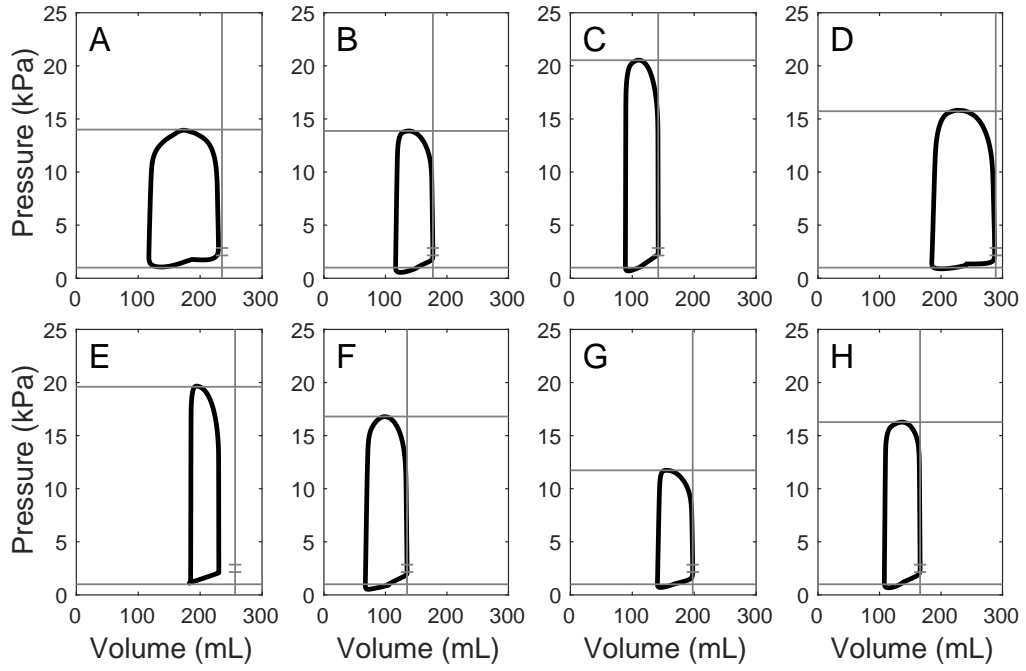


Figure 2.3 Left ventricular pressure-volume loops for the eight human patients.

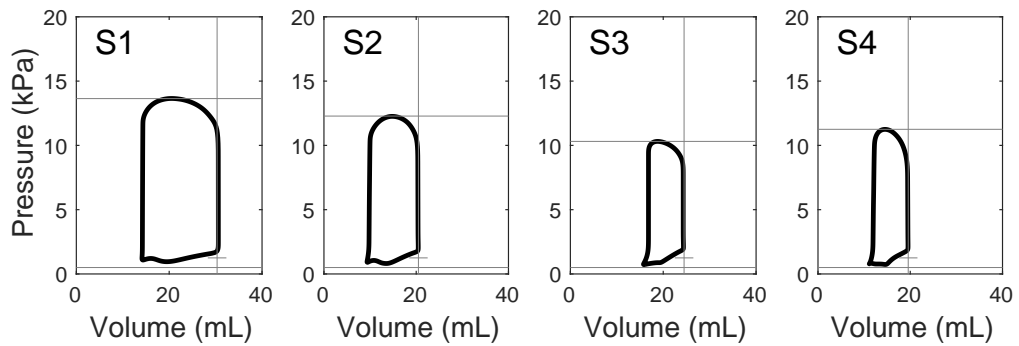


Figure 2.4 Left ventricular pressure-volume loops for the four canine subjects.

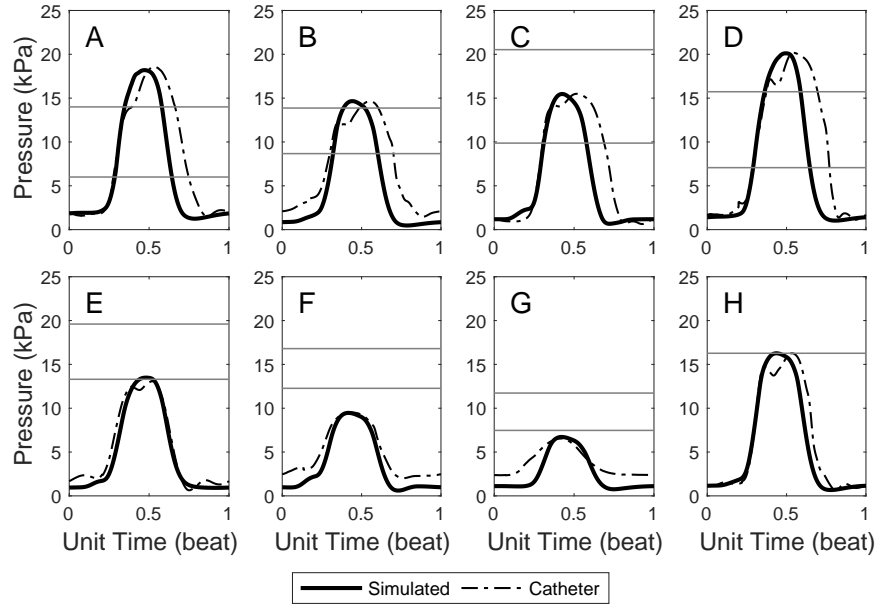


Figure 2.5 Validation of the simulated left ventricular pressure curves for the eight human patients with catheter data after optimizing based on the peak catheter pressure. Gray lines show cuff measurement systolic and diastolic pressures - only catheter pressure was available as the reference for Patient H.

differed from peak left ventricular catheter pressure by an average of 41%. Substituting the LV catheter pressure for cuff pressure as the optimization input reduced RMSE by an average of 31%; patient E error decreased by 69% (Figure 2.5). It must be noted that catheter measurements are not routinely performed on heart failure patients. We tried several different approaches to get an effective simulated pressure time-course in the absence of reliable, invasive pressure data; we discuss these approaches in detail in the Supplement. The approach that gave the best result was to optimize the patients using the cuff systolic pressure first and then replacing the MAP and Sf_{act} for all patients with an average value (Figure 2.6). This method reduced the RMSE error for most patients except for patient G and H (Table 2.6).

Since cuff pressure was not available for the canine subjects, catheter data was used as a direct optimization input. This led to a lower average RMSE than for the non-invasive

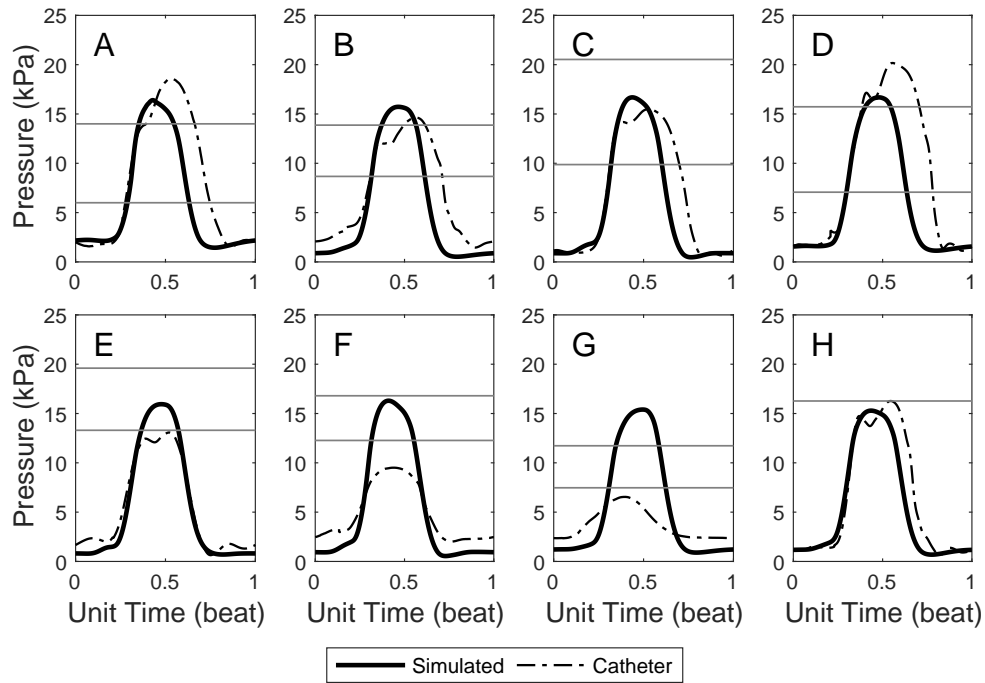


Figure 2.6 Validation of the simulated left ventricular pressure curves for the eight human patients with catheter data after tuning the optimized results with the average MAP and S_{fact} . Gray lines show cuff measurement systolic and diastolic pressures - only catheter pressure was available as the reference for Patient H.

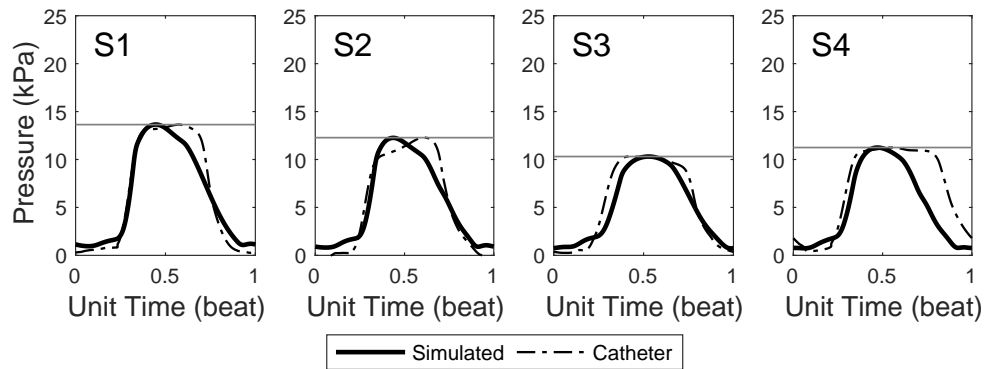


Figure 2.7 Validation of the simulated left ventricular pressure curves for the the four canine subjects with catheterized in-vivo pressure data. Gray line shows reference catheter pressure.

Table 2.6 RMSE between both human and canine model and catheter data when either cuff (with or without using the mean values of MAP and Sf_{act}) or catheter pressure is used as an optimization input.

Subject/ Patient	Cuff (kPa)	Mean (kPa)	Cath (kPa)
A	4.07	2.90	2.41
B	2.66	2.57	2.75
C	2.85	2.53	2.78
D	4.59	4.08	3.28
E	3.11	1.53	0.97
F	3.48	3.29	1.43
G	2.79	4.44	1.39
H	1.42	1.55	1.42
S1	-	-	1.30
S2	-	-	1.41
S3	-	-	1.11
S4	-	-	2.72

human patient results (1.6 kPa vs. 3.12 kPa, Fig. 2.7). One of the largest contributors to the calculated RMSE values was inaccuracy in the total time of cardiac tissue activation. This value was not a parameter in the optimization, since there was no available patient data to evaluate it against, and thus remained at the typical reference value. Table 2.6 shows the RMSE values for each subject and each patient when optimized with cuff and catheter pressure.

2.6.2 Finite-element model results

Material properties for four canine subjects were fitted using a left-ventricular passive inflation simulation in Continuity (Table 2.7). The optimized values for all subjects were notably dissimilar from the reference values. S1 had much different values than the other subjects, likely caused by its significantly greater chamber volume. The average least squares error was 0.21, ranging from 0.09 to 0.30. Figure 2.8 shows the resulting unloaded meshes and EDPVR curves for all four subjects.

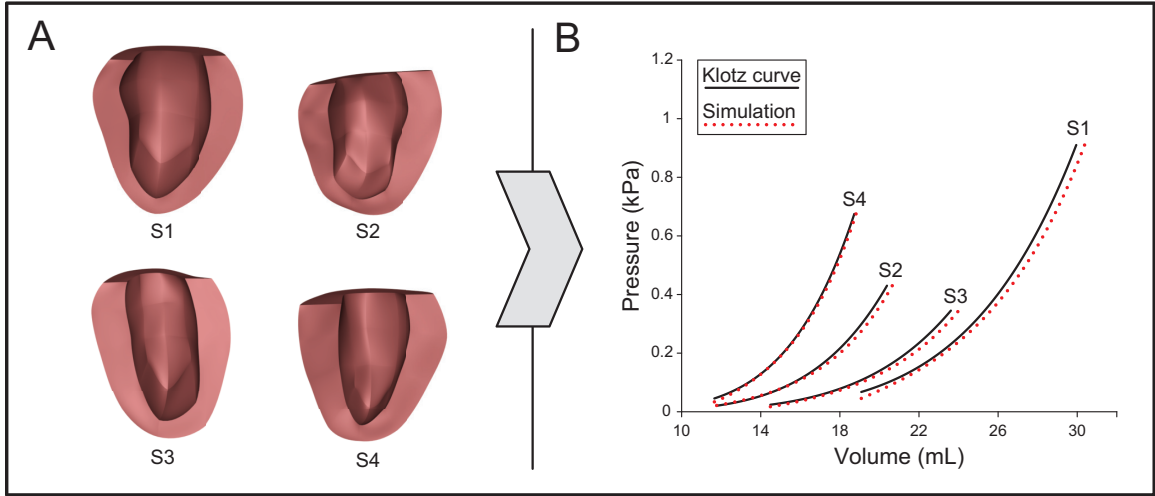


Figure 2.8 Results from simulated inflations of four canine left ventricles. (A) The final unloaded meshes. (B) Comparison of the optimized simulated pressure-volume curves to the Klotz curves (Klotz et al., 2006).

The largest impediment to fit was the allowed EDV convergence error for the estimation of the undeformed ventricle geometry. The average solution took 76 hrs with 1277 evaluations, each requiring 2-3 inflation deflation iterations; however the number of required unique evaluations varied widely between 374 and 3092, with repeat configurations used the previously logged result for efficiency.

Table 2.7 Optimized coefficients from Eq. 2.9 and Klotz curve (Klotz et al., 2006) fit for each canine subject.

Subject	a (kPa)	a_f (kPa)	b -	b_f -	Objective -
<i>ref</i>	1.5	15	8	15	-
S1	1.6	5.1	7.3	4.5	0.30
S2	0.1	11.1	4	14.3	0.22
S3	0.3	6.8	4.3	12.7	0.09
S4	0.4	4.8	4.5	43.5	0.21

2.7 Discussion

Our results showed that the proposed optimization-based tuning framework avoids many of the issues inherent to manual tuning. Circulatory and finite-element models were tuned for individuals with widely-varied parameters, but acceptable solutions were found for all of them. It would be very time-consuming and tedious to manually tune these models from a standard set of assumed parameter values in each case without considerable experience. In addition, the manual process does not ensure repeatability of the parameter results. Evaluation of the manual tuning performed by [Krishnamurthy et al. \(2013\)](#) on CircAdapt models of the same patients used in this study resulted in an average objective of $2.42e-3$, 97% higher than even the worst result from our method; pressure was the largest error contributor. In addition, the manual process was significantly slower, with each patient requiring up to 3 to 4 days of manual tuning. Our optimized parameter values were also very different between individuals, suggesting that immediate local optima were avoided. We showed how the adaptation of idealized reference values to patient-specific data can be seamlessly integrated, thereby allowing for missing data.

One of the main insights that we obtained during implementation of the framework is that the objective function for the circulation model optimization had to be carefully selected. Just including Pmax and EDV alone as part of the objective function were not enough to obtain consistent optimization results. Without the addition of the other penalties, primarily from reference values, the resulting P-V loops were highly unrealistic in both shape and position. We also found that an appropriate QRS duration value was vital to avoid model artifacts caused by incorrect fill timing. In support of our hybrid global approach, early searches for local CircAdapt solutions produced unusable results; this shows that some of the previous methods in the literature, such as NMS and Levenberg-Marquardt, may not be appropriate for certain patient-specific parameters in our optimization. Generally, local optimizers that are heavily influenced by initial assumptions offer improved convergence and precision; however, they can also increase the likelihood of issues due to

sensitive parameters common in PSM which can easily be initialized in a non-global basin-of-attraction. We were also surprised that the optimized canine material parameters in the FEA model all converged to apparently reasonable values with the initially-assumed loose bounds, suggesting that it is possibly a convex problem or that typical material parameters give relatively good results for a wide variety of individuals.

Though the proposed framework addressed many of the issues currently impeding the use of patient-specific cardiovascular models, there are still some key limitations to its application. The first is that the use of noninvasive data imposes limitations on accuracy and data acquisition. However, requiring invasive procedures reduces the value of the framework as compared to more traditional explorative methodologies. The most efficient response is to determine the data sources which are most sensitive and justify the most effort to capture accurately. In the circulatory optimization, k_{MAP} , Sf_{act} , and k_{LV} were the most sensitive parameters; all had mean-normalized standard deviations less than half the value of any other parameter. The values of these parameters are strongly correlated with P_{max} and EDV , which is not surprising as those metrics were most heavily weighted in the objective, meaning that the accuracy of those reference measurements will have a large effect on the results of the optimization.

We found that non-invasive measures of P_{max} were especially unreliable, and this has also been documented in the literature (Raamat et al., 2013). Obtaining pressure through catheterization is currently ideal for data reliability, but improvements in non-invasive measurement methods are necessary to enable the broader application of PSM. Along with the approach of averaging MAP and Sf_{act} discussed in the Results section, we also tried using diastolic cuff pressure as a reference for aortic diastolic pressure. However, none of these methods had a lower RMSE compared to the catheterized pressure measurements. These results can be found in the Supplemental section.

Another limitation is that it is generally impossible to prove that a global optimum has been found for non-convex non-analytical problems, so there is always the potential for a

slightly better tuned result. It is also still necessary that an appropriate objective function be manually constructed to evaluate model fit, which can often be surprisingly difficult. This problem decreases in significance as the specific application of a model becomes more widespread; in such cases a "state-of-the-art" objective function and parameter bounds can be shared among researchers and clinicians without requiring local expertise.

In summary, this framework can facilitate the widespread use of patient-specific or subject-specific models by enabling tuning from non-invasive data. The optimization methods employed are resource efficient and easily scalable to the needs and computational capacity of the application. Using an optimization framework, the information learned in the medical community can be easily and reliably distributed, making it relatively easy to tune a new patient model in a clinical environment compared with current manual methods. Finally, the framework is also usable in a research setting, where a major concern in cross-species research is maintaining a consistent protocol. By tuning both human and canine circulatory models with no modifications to the implementation besides reference parameter values we demonstrate that this concern can be naturally addressed. This work can be used in cross-species research and contribute to improved treatment of CVD.

2.8 References

- Agoshkov, V., Quarteroni, A., and Rozza, G. (2006). A mathematical approach in the design of arterial bypass using unsteady Stokes equations. *Journal of Scientific Computing*, 28(2-3):139–165.
- Arnold, S. V., Decker, C., Ahmad, H., Olabiyi, O., Mundluru, S., Reid, K. J., Soto, G. E., Gansert, S., and Spertus, J. A. (2008). Converting the informed consent from a perfunctory process to an evidence-based foundation for patient decision making. *Circulation: Cardiovascular Quality and Outcomes*, 1:21–28.
- Arts, T., Delhaas, T., Bovendeerd, P., Verbeek, X., and Prinzen, F. W. (2005). Adaptation to mechanical load determines shape and properties of heart and circulation: the CircAdapt model. *American Journal of Physiology: Heart and Circulatory Physiology*, 288:H1943–H1954.

- Baillargeon, B., Rebelo, N., Fox, D. D., Taylor, R. L., and Kuhl, E. (2014). The Living Heart Project: A robust and integrative simulator for human heart function. *European Journal of Mechanics - A/Solids*, 48:38–47.
- Camara, O., Mansi, T., Pop, M., Rhode, K., Sermesant, M., and Young, A., editors (2014). *Statistical Atlases and Computational Models of the Heart: Imaging and Modelling Challenges*. Springer.
- Clay, S., Alfakih, K., Radjenovic, A., Jones, T., Ridgway, J. P., and Sinvananthan, M. U. (2006). Normal range of human left ventricular volumes and mass using steady state free precession MRI in the radial long axis orientation. *Magnetic Resonance Materials in Physics, Biology and Medicine*, 19(1):41–45.
- CMRG (2015). Continuity 6.4.
- Dugdale, D. C., Epstein, R., and Pantilat, S. Z. (1999). Time and the Patient-Physician Relationship. *Journal of General Internal Medicine*, 14(Supplement 1):S34–S40.
- Ellwein, L. M., Pope, S. R., Xie, A., Batzel, J., Kelley, C. T., and Olufsen, M. S. (2013). Modeling cardiovascular and respiratory dynamics in congestive heart failure. *Mathematical Biosciences*, 241:56–74.
- Ennis, D. B. (2004). *Assessment of Myocardial Structure and Function Using Magnetic Resonance Imaging*. PhD thesis, Johns Hopkins University.
- Ferrario, M., Chiodini, P., Chambless, L. E., Cesana, G., Vanuzzo, D., Panico, S., Sega, R., Pilotto, L., Palmieri, L., and Giampaoli, S. (2005). Prediction of coronary events in a low incidence population. Assessing accuracy of the CUORE Cohort Study prediction equation. *International Journal of Epidemiology*, 34:413–421.
- Gaziano, T. A., Steyn, K., Cohen, D. J., Weinstein, M. C., and Opie, L. H. (2005). Cost-effectiveness analysis of hypertension guidelines in South Africa: Absolute risk versus blood pressure level. *Circulation*, 112:3569–3576.
- Hardy, H. H., Collins, R. E., and Calvert, R. E. (1982). A digital computer model of the human circulatory system. *Medical and Biological Engineering and Computing*, 20(5):550–564.
- Hendel, R. C., Patel, M. R., Allen, J. M., Min, J. K., Shaw, L. J., Wolk, M. J., Douglas, P. S., Kramer, C. M., Stainback, R. F., Bailey, S. R., Doherty, J. U., and Brindis, R. G. (2013). Appropriate use of cardiovascular technology. *Journal of the American College of Cardiology*, 61(12):1305–1317.
- Hess, E. P., Knoedler, M. A., Shah, N. D., Kline, J. A., Breslin, M., Branda, M. E., Pencille, L. J., Asplin, B. R., Nestler, D. M., Sadosty, A. T., Stiell, I. G., Ting, H. H., and Montori, V. M. (2012). The chest pain choice decision aid: A randomized trial. *Circulation: Cardiovascular Quality and Outcomes*, 5:251–259.

- Heusinkveld, M., Reesink, K., Arts, T., Huberts, W., and Delhaas, T. (2009). Use of vascular adaptation in response to mechanical loading facilitates personalisation of a one-dimensional pulse wave propagation model. *Artery Research*, 20:79–80.
- Holzapfel, G. A. and Ogden, R. W. (2009). Constitutive modelling of passive myocardium: a structurally based framework for material characterization. *Philosophical Transactions of the Royal Society: Series A*, 367(1902):3445–3475.
- Hooke, R. and Jeeves, T. A. (1961). “Direct Search” Solution of Numerical and Statistical Problems. *Journal of the ACM*, 8(2):212–229.
- Institute of Laboratory Animal Resources (ILAR) (1996). *Guide for the care and use of laboratory animals*.
- Kerckhoffs, R. C. P., Lumens, J., Vernooij, K., Omens, J. H., Mulligan, L. J., Delhaas, T., Arts, T., McCulloch, A. D., and Prinzen, F. W. (2008). Cardiac resynchronization: Insight from experimental and computational models. *Progress in Biophysics and Molecular Biology*, 97(2-3):543–561.
- Klotz, S., Hay, I., Dickstein, M. L., Yi, G.-H., Wang, J., Maurer, M. S., Kass, D. A., and Burkhoff, D. (2006). Single-beat estimation of end-diastolic pressure-volume relationship: a novel method with potential for noninvasive application. *American Journal of Physiology: Heart and Circulatory Physiology*, 291(1):H403–H412.
- Kovalova, S., Necas, J., and Vespalec, J. (2006). What is a “normal” right ventricle? *European Journal of Echocardiography*, 7(4):293–297.
- Krishnamurthy, A., Coppola, B., Tangney, J., Kerckhoffs, R. C. P., Omens, J. H., and McCulloch, A. D. (2016). A Microstructurally Based Multi-Scale Constitutive Model of Active Myocardial Mechanics. In *Structure-Based Mechanics of Tissues and Organs*, chapter 3, pages 439–460.
- Krishnamurthy, A., Villingco, C., Beck, A., Omens, J., and McCulloch, A. (2015). Left Ventricular Diastolic and Systolic Material Property Estimation from Image Data: LV Mechanics Challenge. *Statistical Atlases for Computerized Models of the Heart*, 8896:63–73.
- Krishnamurthy, A., Villongco, C. T., Chuang, J., Frank, L. R., Nigam, V., Belezouli, E., Stark, P., Krummen, D. E., Narayan, S., Omens, J. H., McCulloch, A. D., and Kerckhoffs, R. C. P. (2013). Patient-specific models of cardiac biomechanics. *Journal of Computational Physics*, 244:4–21.
- Lang, R. M., Bierig, M., Devereux, R. B., Flachskampf, F. A., Foster, E., Pellikka, P. A., Picard, M. H., Roman, M. J., Seward, J., Shanewise, J., Solomon, S., Spencer, K. T., St. John Sutton, M., and Stewart, W. (2006). Recommendations for chamber quantification. *European Journal of Echocardiography*, 7(2):79–108.

- Leong, X. F., Ng, C. Y., and Jaarin, K. (2015). Animal Models in Cardiovascular Research: Hypertension and Atherosclerosis. *BioMed Research International*, 2015.
- Lim, E., Dokos, S., Lovell, N. H., Cloherty, S. L., Salamonsen, R. F., Mason, D. G., and Reizes, J. A. (2010). Parameter-Optimized Model of Cardiovascular-Rotary Blood Pump Interactions. *IEEE Transactions on Biomedical Engineering*, 57(2):254–266.
- Maddox, T. M., Chan, P. S., Spertus, J. A., Tang, F., Jones, P., Ho, P. M., Bradley, S. M., Tsai, T. T., Bhatt, D. L., and Peterson, P. N. (2014). Variations in coronary artery disease secondary prevention prescriptions among outpatient cardiology practices: Insights from the NCDR (National Cardiovascular Data Registry). *Journal of the American College of Cardiology*, 63(6):539–546.
- Marsden, A. L., Feinstein, J. A., and Taylor, C. A. (2008). A computational framework for derivative-free optimization of cardiovascular geometries. *Computer Methods in Applied Mechanics and Engineering*, 197(21-24):1890–1905.
- MathWorks (2017). MATLAB R2017b.
- Mehta, R. H., Peterson, E. D., and Califf, R. M. (2007). Performance Measures Have a Major Effect on Cardiovascular Outcomes: A Review. *American Journal of Medicine*, 120:398–402.
- Milani-Nejad, N. and Janssen, P. M. L. (2014). Small and large animal models in cardiac contraction research: advantages and disadvantages. *Pharmacology and Therapeutics*, 141(3):235–249.
- Nallamotheu, B. K., Normand, S. L. T., Wang, Y., Hofer, T. P., Brush, J. E., Messenger, J. C., Bradley, E. H., Rumsfeld, J. S., and Krumholz, H. M. (2015). Relation between door-to-balloon times and mortality after primary percutaneous coronary intervention over time: A retrospective study. *The Lancet*, 385(9973):1114–1122.
- Nauser, T. D. and Stites, S. W. (2001). Diagnosis and treatment of pulmonary hypertension. *American Family Physician*, 63(9):1789–1798.
- Neal, M. L. and Bassingthwaite, J. B. (2007). Subject-specific Model Estimation of Cardiac Output and Blood Volume During Hemorrhage. *Cardiovascular Engineering*, 7(3):97–120.
- Niederer, S. A., Fink, M., Noble, D., and Smith, N. P. (2009). A meta-analysis of cardiac electrophysiology computational models. *Experimental Physiology*, 94(5):486–495.
- Olansen, J. B., Clark, J. W., Khoury, D., Ghorbel, F., and Bidani, A. (2000). A Closed-Loop Model of the Canine Cardiovascular System That Includes Ventricular Interaction. *Computers and Biomedical Research*, 33(4):260–295.
- Piper, M. A., Evans, C. V., Burda, B. U., Margolis, K. L., O’Connor, E., and Whitlock, E. P. (2015). Diagnostic and predictive accuracy of blood pressure screening methods

- with consideration of rescreening intervals: A systematic review for the U.S. Preventive Services Task Force. *Annals of Internal Medicine*, 162(3):192–204.
- Raamat, R., Talts, J., Jagomägi, K., and Kivastik, J. (2013). Accuracy of some algorithms to determine the oscillometric mean arterial pressure: A theoretical study. *Blood Pressure Monitoring*, 18:50–56.
- Roth, G. A., Huffman, M. D., Moran, A. E., Feigin, V., Mensah, G. A., Naghavi, M., and Murray, C. J. L. (2015). Global and regional patterns in cardiovascular mortality from 1990 to 2013. *Circulation*, 132(17):1667–1678.
- Shi, Y. and Eberhart, R. (1998). A modified particle swarm optimizer. In *IEEE International Conference on Evolutionary Computation*, pages 69–73.
- Shortliffe, E. H., Buchanan, B. G., and Feigenbaum, E. A. (1979). Knowledge engineering for medical decision making: A review of computer-based clinical decision aids. Technical report, Stanford University Computer Science Department.
- Smith, N., de Vecchi, A., McCormick, M., Nordsletten, D., Camara, O., Frangi, A. F., Delingette, H., Sermesant, M., Relan, J., Ayache, N., Krueger, M. W., Schulze, W. H. W., Hose, R., Valverde, I., Beerbaum, P., Staicu, C., Siebes, M., Spaan, J., Hunter, P., Weese, J., Lehmann, H., Chapelle, D., and Rezavi, R. (2011). euHeart: personalized and integrated cardiac care using patient-specific cardiovascular modelling. *Interface Focus*, 1(3):349–364.
- Stacey, D., Légaré, F., Lewis, K., Barry, M. J., Bennet, C. J., Eden, K. B., Holmes-Rovner, M., Llewellyn-Thomas, H., Lyddiatt, A., Thompson, R., and Trevena, L. (2017). Decision aids for people facing health treatment or screening decisions. Technical Report 4.
- Tange, O. (2011). GNU Parallel - The Command-Line Power Tool. *login: The USENIX Magazine*, 36(1):42–47.
- Ting, H. H., Chen, A. Y., Roe, M. T., Chan, P. S., Spertus, J. A., Nallamothu, B. K., Sullivan, M. D., DeLong, E. R., Bradley, E. H., Krumholz, H. M., and Peterson, E. D. (2010). Delay from symptom onset to hospital presentation for patients with non-ST-segment elevation myocardial infarction. *Archives of Internal Medicine*, 170(20):1834–1841.
- Vukanovic-Criley, J. M., Criley, S., Warde, C. M., Boker, J. R., Guevara-Matheus, L., Churchill, W. H., Nelson, W. P., and Criley, J. M. (2006). Competency in cardiac examination skills in medical students, trainees, physicians, and faculty: a multicenter study. *Archives of internal medicine*, 166(6):610–616.
- Wang, V. Y., Lam, H. I., Ennis, D. B., Cowan, B. R., Young, A. A., and Nash, M. P. (2009). Modelling passive diastolic mechanics with quantitative MRI of cardiac structure and function. *Medical Image Analysis*, 13(5):773–784.

Wilson, P. W. F., D’Agostino, R. B., Levy, D., Belanger, A. M., Silbershatz, H., and Kannel, W. B. (1998). Prediction of coronary heart disease using risk factor categories. *Circulation*, 97:1837–1847.

Yoshimura, M., Yasue, H., Okumura, K., Ogawa, H., Jougasaki, M., Mukoyama, M., Nakao, K., and Imura, H. (1993). Different secretion patterns of atrial natriuretic peptide and brain natriuretic peptide in patients with congestive heart failure. *Circulation*, 87(2):464–469.

Zoghbi, W. A. (2016). Quantifying Valvular Regurgitation. In *ACC Middle East Conference*.

2.9 Appendix: Supplemental Methods and Validation

Performance of the circulatory model optimization was highly dependent on the quality of the patient-specific pressure data. In the absence of reliable pressure data, we tried different methods that can be used to still obtain a patient-specific pressure time-course. This section outlines three other methods with corresponding validation plots comparing their results with catheter data - the highest quality data available. Table 2.8 contains the RMSE between the model and catheter data for all approaches.

The original method discussed in the paper uses systolic cuff pressure as a target value for simulated peak LV pressure. Though the resulting pressure errors were within 0.53% of the reference cuff pressure, a more fundamental issue was identified regarding the limitations of cuff pressure accuracy. Figure 2.9 shows the resulting model LV pressure curves of the initial optimization formulation validated against experimentally-obtained catheter data. The peak pressure values differ significantly, leading to a high average RMSE of 3.12 kPa.

To minimize the variance in cuff pressure readings, we used the average optimized values of MAP and Sf_{act} - the two parameters with the strongest effect on P_{max} - for all patients. That result can be seen in the paper (Fig. 2.6).

Another approach we investigated was to use cuff diastolic pressure as the reference value for simulated aortic diastolic pressure, instead of optimizing for peak LV pressure; the form of the objective formulation was unchanged. The result can be seen in Figure 2.10. This approach improved some patient models (C and G) and negatively impacted others

Table 2.8 RMSE between human model and catheter data when either cuff (with or without using the mean values of MAP and Sf_{act} in \mathbf{x}) or catheter pressure is used as an optimization input and when modeled aortic diastolic pressure is optimized against cuff diastolic pressure.

Patient	Cuff (kPa)	Mean (kPa)	Aorta (kPa)	Cath (kPa)
A	4.07	2.90	5.59	2.41
B	2.66	2.57	2.97	2.75
C	2.85	2.53	2.49	2.78
D	4.59	4.08	6.07	3.28
E	3.11	1.53	3.66	0.97
F	3.48	3.29	6.02	1.43
G	2.79	4.44	1.97	1.39
H	1.42	1.55	1.42	1.42

(e.g. A and F), but increased average RMSE by 21%. This implies that diastolic cuff pressure is no more reliable of a measurement than systolic cuff pressure.

Finally, we performed the optimization using the LV catheter data directly as a reference for peak LV pressure. In Figure 2.5, it can be seen that the model and optimization framework are capable of generating realistic and accurate LV pressure curves given a reliable value for peak pressure. Improvements to non-invasive blood pressure measurement techniques are needed to ensure results of this quality.

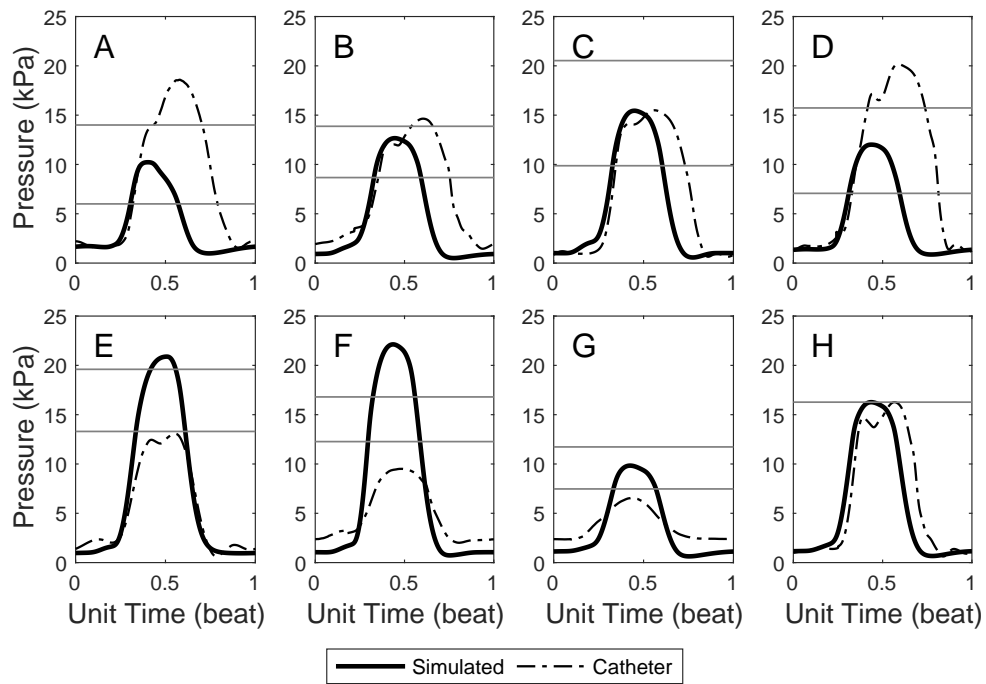


Figure 2.9 Validation of the simulated left ventricular pressure curves optimized using systolic cuff pressure for the eight human patients with catheter data. Gray lines show cuff measurement systolic and diastolic pressures - only catheter pressure was available as the reference for Patient H.

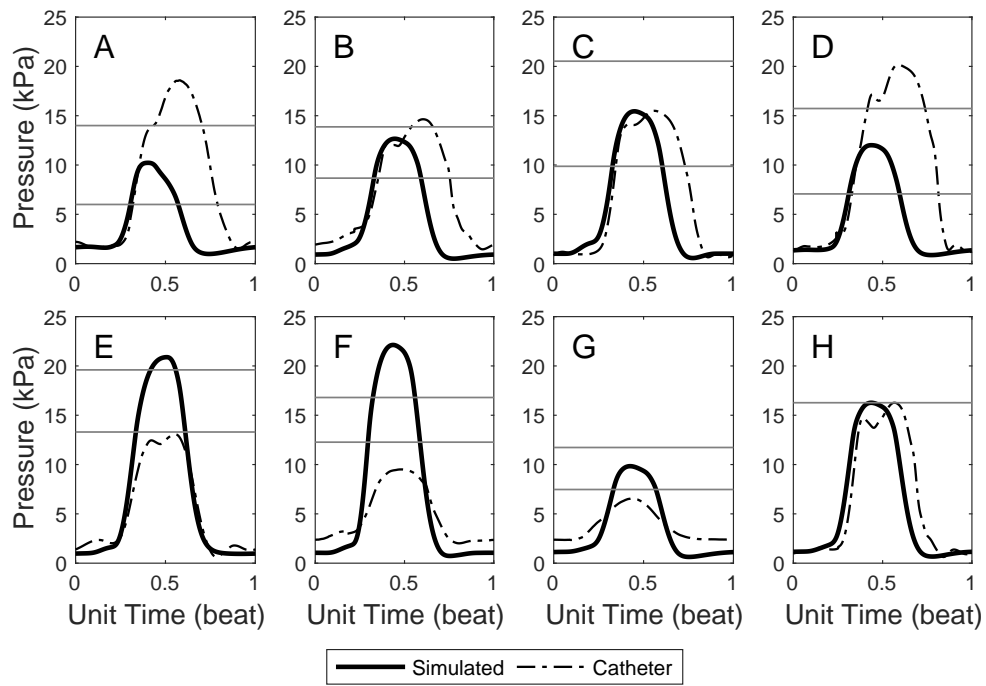


Figure 2.10 Validation of the simulated left ventricular pressure curves for the eight human patients with catheter data after optimizing with measured diastolic cuff pressure as a reference for aortic diastolic pressure. Gray lines show cuff measurement systolic and diastolic pressures - only catheter pressure was available as the reference for Patient H.

CHAPTER 3. OPTIMIZATION FRAMEWORK FOR PATIENT-SPECIFIC MODELING UNDER UNCERTAINTY

This paper is in review for *The International Journal for Numerical Methods in Biomedical Engineering*. It was authored by Joshua Mineroff, Balaji Sessa Sarath Pokuri, Adarsh Krishnamurthy, and Baskar Ganapathysubramanian. I was responsible for developing, implementing, and testing the sampling and optimization framework as well as for writing the majority of the manuscript. Balaji contributed the surrogate generation code and most of the matching section of the paper. Adarsh informed the scope of the paper and supported relevance to the field of cardiac modeling. Baskar helped create the approach and advised on methodological decisions.

3.1 Abstract

Tuning of computerized models relies on data that is often unreliable and ill-suited to a deterministic approach. We develop an optimization-based uncertainty quantification framework for probabilistic model tuning that discovers distributions of model inputs which generate target output distributions. Probabilistic sampling is performed using a model surrogate for computational efficiency and a general distribution parameterization is used to describe each input. The approach is tested on four patient-specific modeling examples using CircAdapt, a cardiac circulatory model. Three examples are synthetic, aiming to match the output distributions generated using known reference input data distributions, while the fourth example uses real-world patient data for the output distributions. Our results demonstrate accurate reproduction of the target output distributions, with accurate

recreation reference inputs for the three synthetic examples. Although further testing is needed to prove generalizability of the method, it appears suitable for the tuning of models with uncertain data.

3.2 Acknowledgements

This research was supported in part by NIH grant 1 R01 HL131753 (Krishnamurthy) and by NSF grant 1750865 (Krishnamurthy), and by the Joseph C. and Elizabeth A. Anderlik Professorship at Iowa State University (Mineroff). We would also like to show our gratitude to Dr. Judy Vance at Iowa State University for her extraordinary support.

3.3 Introduction

Computational models can be used to more efficiently and thoroughly understand a complex system than experiments at reduced cost. While many aspects of these simulations are idealized or analytically formulated, certain components require manual or automated tuning of model parameters to accurately capture the modeled system. The values of these parameters are often determined using experimental or reference data, either directly or indirectly via dependent model values. However, available data is often unreliable; this uncertainty impedes consistent tuning and must be accounted for to fully determine the accuracy and validity of a result.

There are many ways to control or understand variability, but methods can be broadly divided into the categories of validation and analysis. Validation uses reliable data, extrinsic to the model, to test for model correctness. This can provide exact accuracy measurements, but redundant experimental data may not be available and the need for experimental data negates a key benefit of physically-representative models. Sensitivity and uncertainty analysis aim to characterize the variability of a model intrinsically, and a comparison of these mathematical methods was performed by [Iman and Helton \(1988\)](#). Sensitivity analysis looks at the effect of each individual variable on the model to determine which parameters

are most important, which helps to focus data collection to where it will be most valuable. Uncertainty analysis, or uncertainty quantification (UQ), is the direct characterization of model uncertainty resulting from uncertain inputs. Instead of obtaining a model output and judging its accuracy, UQ provides a range of possible output values with the distribution of their occurrence. [Walker et al. \(2003\)](#) investigated the conceptual integration of uncertainty into models intended for decision support to help the user make informed choices. Mathematical methods of UQ are not especially new, but the transition to domain-specific application has been slow.

One growing application of uncertainty classification in models is the use of patient-specific modeling (PSM) in the study and practice of medicine. PSM is the use of patient-specific data to individualize biomedical models. Information derived from such models can inform medical interventions by providing clinicians with more accurate and comprehensive diagnostic information as well as the predicted effects of different treatment modalities ([Neal and Kerckhoffs, 2009](#)); it also introduces the potential to automate aspects of clinical decision making, improving treatment consistency. Computational PSM continues to rise in importance as the understanding of diseases and availability of diagnostic and treatment options becomes more complex, and practicing physicians have to rely more on specialists outside their area of expertise ([Shortliffe et al., 1979](#)). Additionally, a significant level of training is currently required to initialize and operate them. Models used for PSM continue to increase in complexity, magnifying uncertainties in model inputs. However, tuning approaches are often still deterministic and do not account for this variability ([Krishnamurthy et al., 2013](#); [Ellwein et al., 2013](#); [Reinbolt et al., 2008](#)).

Treatment of cardiovascular disease (CVD), the leading cause of death in developed countries ([Roth et al., 2015](#)), can significantly benefit from PSM and some such models are already being tested in clinical settings ([Niederer et al., 2009](#); [Kerckhoffs et al., 2008](#)). The highly sophisticated models needed for patient-specific cardiovascular modeling rely on a large number of uncertain data and can be expensive to validate. UQ has been applied

to cardiovascular model tuning, though there is still no standard approach. [Huberts et al. \(2018\)](#) propose a method to make uncertain cardiovascular models more useful for diagnosis and intervention based largely on sensitivity analysis. [Sankaran and Marsden \(2011\)](#) perform UQ for a variety of geometric cardiovascular models using a stochastic collocation approach. [Xiu and Sherwin \(2007\)](#) used a generalized polynomial chaos expansion method for UQ in a 1D model. Further deployment depends on the development of efficient and consistent model tuning methodologies.

We propose a general framework for probabilistic model tuning with uncertainty quantification and test it using a cardiovascular circulatory model, CircAdapt ([Arts et al., 2005](#)). The CircAdapt model is used to find input parameter distributions such that expected model output distributions match those of experimentally measured non-invasive patient-specific data. Parameterization of model variable distributions is done without any assumptions of the form of those distributions. Since CircAdapt is a deterministic model, probabilistic sampling of the model inputs was needed to get a distribution of outputs. To make the necessary volume of evaluations computationally tractable, a surrogate model was built using the PARyOpt framework ([Pokuri et al., 2018](#)). The combination of these techniques supports accurate, efficient uncertainty analysis of expensive models.

The main contributions of this work include the development of:

1. An optimization framework for uncertainty quantification of model parameters.
2. A methodology for the estimation of uncertain patient-specific biophysical model parameters.
3. An efficient implementation of input distribution parameterization using deterministic surrogates.

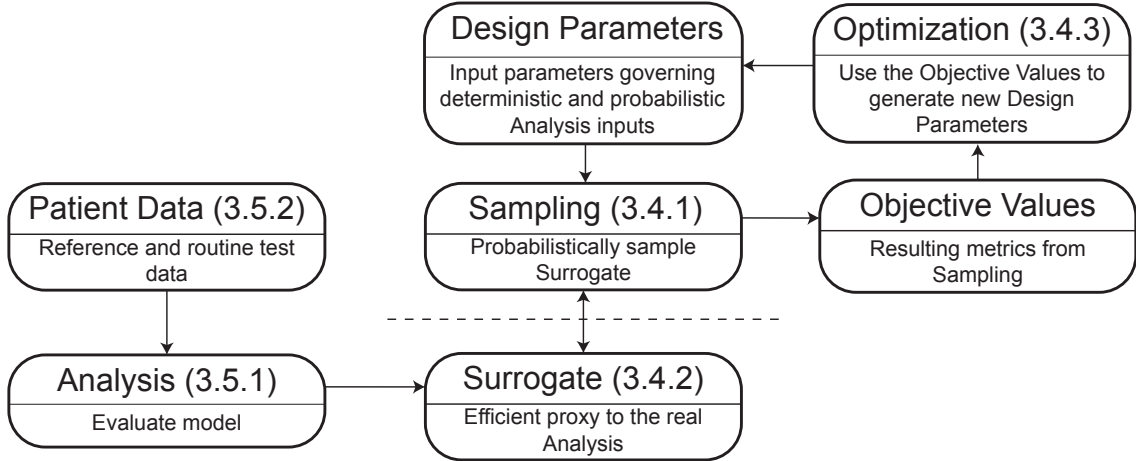


Figure 3.1 A flowchart of the Design Under Uncertainty (DUU) framework.

3.4 Framework for Design Under Uncertainty

Inverse models are tuned by determining model input parameters such that model outputs match with available data. The error inherent in this data mean that a deterministic approach is not ideal. Our Design Under Uncertainty framework (DUU, Fig. 3.1) is designed to tune computerized models using uncertain data and builds on the methodology developed by [Mineroff et al. \(2018\)](#). Specifically, the goal of the framework is to determine the distribution of model inputs that match expected model output distributions. The primary components of the framework are the probabilistic sampling method, the efficient surrogate, the optimizer, and the original model.

3.4.1 Probabilistic parameterization and sampling

Probabilistic variables require more parameters to fully characterize than deterministic variables. This necessitates the selection and development of an appropriate distribution to accurately parameterize a probabilistic variable. Certain distributions can be described with as few as two parameters per variable, e.g. mean and standard deviation for a normal distribution; however, there are many different probability distributions used to describe

uncertainty, even in the limited case of patient data (Gordon et al., 1983; Kuikka et al., 1974). General parameterization schemas allow for any of these distributions to be discovered when tuning the model. The proposed framework describes the distribution of each model variable with parameter values representing probabilistically-uniform variable values on the CDF. This approach supports a wide range of distributions, including deterministic variables, and trivial parameterization refinement for more sensitive variables. Since $p = 0$ and $p = 1$ correspond with the values that are probabilistically guaranteed to be the lower or upper bound of x they tend to attract towards negative and positive infinity, respectively. To avoid this, we confine our representation and sampling of the CDF between $p = 0.01$ and $p = 0.99$.

There are a few ways to implement the proposed distribution parameterization for a model variable \mathbf{x} . The most straightforward method is to have N parameters that directly represent the values of \mathbf{x} at evenly spaced probabilities on the CDF. To ensure a valid solution, each x_n is bounded by the same bounds as x and $N - 1$ constraints are required to ensure that the resulting CDF is monotonic. Another approach is for x_1 to directly represent the lower bound of the distribution, while all subsequent parameters represent the increase in \mathbf{x} over a given probability interval. If all parameters starting with x_2 are bounded to be positive, this decreases the required number of constraints per variable to 1 which ensures that the sum of all parameters representing x satisfies the upper bound of the model parameter. Both of these approaches can be effective, but the need for constraints makes them more expensive.

Our approach adds an extra parameter to the description of each model variable to remove the requirement for constraints. In this approach, x_1 represents the value corresponding to $p = 0.01$. An additional $N - 1$ parameters, bounded between 0 and 1, represent the relative sizes of increments between x_1 and x_N . An additional parameter, bounded between 0 and 1, scales the length between x_1 and the upper bound of \mathbf{x} . A value of 0 for this parameter means that $x_N = x_1$, while a value of 1 means that x_N equals the upper

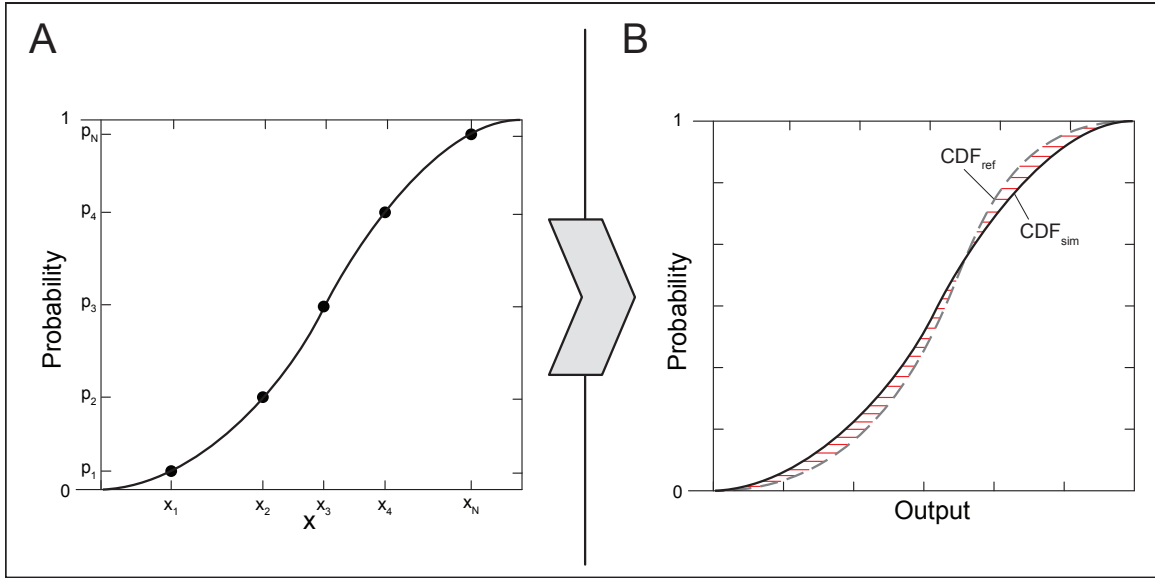


Figure 3.2 A representative example of a tuned model. (A) Parameterization of an input variable distribution, where $n = 5$. (B) Error fitting of the simulated result with a reference CDF.

bound of \boldsymbol{x} . A representation of this parameterization is shown in (Fig. 3.2A). This allows an potential distribution of \boldsymbol{x} to be represented without the need for constraints.

Since many models are deterministic, there is often no way to directly evaluate a probabilistic variable. This necessitates the sampling of deterministic variable values from the described distribution. By Borel’s law of large numbers, a large number of samples evaluated in this way will generate an accurate output distribution. The parameterization previously described has the benefit that arbitrarily accurate probabilistic sampling can be performed cheaply by evaluating model values located probabilistically-uniformly along the CDF. Multiple probabilistic inputs can be sampled in this way, but must be combined in a way that avoids false correlation effects. We take the tensor product of the samples for each input to get a complete set of samples, which assumes that the variables are mutually independent.

3.4.2 Surrogate modeling

Probabilistic models are generally represented in terms of a non-parameterized CDF developed through multiple evaluations using probabilistically represented variables. This complexity means that probabilistic model evaluation is significantly more expensive than that of the same deterministic model. Additionally, each previously deterministic variable now requires multiple parameters for a probabilistic representation – if 20 parameters are used to represent each input distribution, then optimization of a 3 parameter deterministic model expands to a 60 parameter problem. Thus methods need to be devised to reduce the total number of resource-intensive cost function evaluations.

There are several methods available to tackle such high-dimensionality optimization problems. A common technique (Leifsson et al., 2014; Robinson et al., 2008) is to consider a reduced-order model representation for global optimization, which can substantially reduce total optimization cost as the reduced-order cost function is cheaper to evaluate than the original. However, this introduces a potential limitation – when reduced-order models do not exist or have very low fidelity, the high-fidelity optimization is required. Therefore, to take advantage of this technique and ensure broad applicability of the proposed framework, a generalized method is needed to construct a cheap, reduced-order “meta-model” which captures the response surface of the cost function.

There are several techniques to create a meta-model; the most common being interpolation with varying degrees of continuity – this includes splines (Friedman, 1991), polynomial interpolation (De Boor and Ron, 1990), and finally Gaussian processes (Dyn et al., 1986; Fang and Horstemeyer, 2006). In this work, we use Gaussian process modeling to efficiently build the reduced-order surrogate. It should be noted that an efficient meta-model also implies efficient sampling when constructing the meta-model, not just efficient polling. Gaussian processes, like radial basis function based Kriging (Cressie, 1988), offer this advantage over other techniques by providing a natural way to quantify informativeness of different input configurations. Secondly, Gaussian processes absorb all data locations with-

out over-fitting, so the generated surrogate will be an interpolant rather than a regression, preserving the original cost function evaluations.

In this work, we use Kriging to create a meta-model of the cost-function. Kriging is a general interpolation technique based on Gaussian priors and posteriors on functionals aimed at approximating a, typically expensive, ‘oracle’ function. The approximate function is described in terms of the mean and variance of distribution of the functions. Based on this description, an informativeness metric is defined, commonly called the acquisition function; locations with maximum information addition have a large value of acquisition function and vice-versa. The ‘oracle’ function is then evaluated at these extrema of acquisition function and the values are used to construct a posterior distribution. Mathematically, the algorithm can be described as follows:

The surrogate/meta-model is constructed in the form:

$$\tilde{y}(\mathbf{x}) = \sum_{i=1,2,..N} w_i k(\mathbf{x}_i, \mathbf{x}) \quad (3.1)$$

where $k(\mathbf{x}_i, \mathbf{x})$ is a kernel function. The constructed meta-model (mean μ and variance σ), after N function evaluations is given by

$$\mu(\mathbf{x}_{N+1}) = \mathbf{k}^T \mathbf{K}^{-1} \mathbf{y}_{1:N} \quad (3.2)$$

$$\sigma^2(\mathbf{x}_{N+1}) = k(\mathbf{x}_{N+1}, \mathbf{x}_{N+1}) - \mathbf{k}^T \mathbf{K}^{-1} \mathbf{k} \quad (3.3)$$

where

$$\mathbf{K} \bar{w} = \mathbf{y} \quad (3.4)$$

$$\mathbf{K}_{i,j} = k(\mathbf{x}_i, \mathbf{x}_j), \quad i, j \in [1, N] \quad (3.5)$$

$$y_i = y(\mathbf{x}_i), \quad i \in [1, N] \quad (3.6)$$

$$\bar{w} = \{w_i\}, \quad i \in [1, N] \quad (3.7)$$

and

$$\mathbf{k} = \mathbf{k}(\mathbf{x}_{N+1}) = [k(\mathbf{x}_1, \mathbf{x}_{N+1}) k(\mathbf{x}_2, \mathbf{x}_{N+1}) \dots k(\mathbf{x}_N, \mathbf{x}_{N+1})] \quad (3.8)$$

To perform the above tasks, we use an in-house software, PARyOpt (Pokuri et al., 2018), which performs *parallel* cost function evaluations *asynchronously*, enabling multiple simultaneous function evaluations and can be deployed locally or on a HPC cluster, with resilience to hardware failures. It is fully modular and ‘oracle’ function agnostic and it can deal with ‘oracle’ failures – i.e., if the simulation is infeasible at a particular location, it can still assimilate that location with an explicit ‘tag-of-failure’ associated with the infeasible point. This feature of assimilating failed points is particularly handy when infeasibility of evaluation locations cannot be estimated a priori.

3.4.3 Optimization framework

Complex models of real-world systems tend to be multi-modal and highly corrugated. This, combined with the probabilistic model sampling necessary in each evaluation, makes the calculation of gradients intractable and supports a derivative-free approach. We employ a two-step approach; first using particle swarm optimization to perform a global search of the problem space, and finally using pattern search to converge to a precise local optima. The optimization and surrogate sampling for each evaluation is performed using MATLAB (MathWorks, 2017). This methodology and implementation is efficient enough to make local model tuning on a consumer laptop feasible.

The correctness of each model output is calculated using the RMS error between the simulated output inverse-CDF (iCDF) and the predetermined target output iCDF, defined using a combination of patient and reference data (Fig. 3.2B). Since models are often tuned using more than one piece of output data as a target, the objective function needs to allow for the consideration of multiple model output distributions. The selected optimization formulation (Eq. 3.9) supports this by using a linear combination of the output RMS errors.

$$\begin{aligned}
& \arg \min_{\mathbf{x}} \sum_{n=1}^N a_n \sqrt{\frac{1}{M} \sum_{m=1}^M (CDF_{mn}(\mathbf{x}) - rCDF_{mn})} \\
& \text{s.t.} \quad E(f_n(\mathbf{x})) = 0, \text{ for all } n \quad (*\text{Surrogate of ODE solution}), \\
& \quad \quad \quad A\mathbf{x} \leq b \quad (\text{Bounds on } \mathbf{x})
\end{aligned} \tag{3.9}$$

*Note that surrogate accuracy is actually better than an expected value of 0. Pointwise the kriged model is exactly correct at the location, and within some region, of sampled points.

3.5 Circulatory Model

3.5.1 CircAdapt

CircAdapt ([Arts et al., 2005](#)) is a lumped-parameter model of the circulatory system (Fig. 3.3) implemented in MATLAB. It provides detailed information on hemodynamic properties within the heart at any time during the cardiac cycle. We consider the model variables and outputs identified as most important by [Mineroff et al. \(2018\)](#) (Table 3.1) along with select patient data.

Table 3.1 Details and bounds of the different CircAdapt variables affected by \mathbf{x} .

Variable	Description	Lower Bound	Upper Bound	Units	Reference
k_{MAP}	Scaling of mean arterial pressure initially calculated using the '33% formula'	0.8	1.2	-	(Raamat et al., 2013)
k_{LV}	Geometric scaling factor of left ventricular midwall surface area from CircAdapt reference configuration	0.5	2	-	(Clay et al., 2006)
Sf_{act}	Maximum isometric active stress of myofibers	25	200	kPa	
Sf_{pas}	Passive stiffness of myofibers	10	30	kPa	

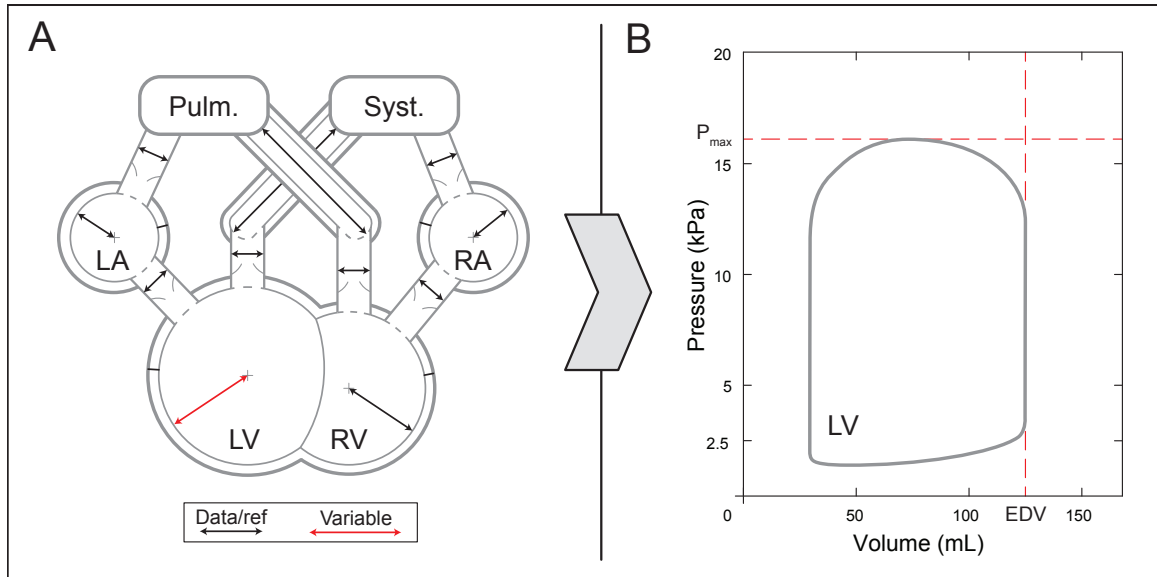


Figure 3.3 A schematic, showing geometric parameters, and output P-V loop, showing the deterministic metrics, of the CircAdapt model. (A) A schematic of the CircAdapt model highlighting key geometric dimensions of major model components. (B) A typical simulated left ventricular (LV) pressure-volume loop showing both metrics. Pulm. = pulmonary circulation; Syst. = systemic circulation; LA = left atrium; RA = right atrium; RV = right ventricle; EDV = end-diastolic volume.

3.5.2 Clinical data

The human patient studied was male, aged (approximately 66 years) with NYHA class III heart failure, dilated cardiomyopathy, and left bundle branch block (LBBB) and enrolled from the Veteran's Administration San Diego Healthcare System (San Diego, CA). Patient gave informed consent to participate in the human subject protocol approved by the institutional review board. Key cardiac measurements were recorded via echocardiogram and routine diagnostic methods.

Table 3.2 Summary of synthetic examples. In Example 2, the bolded distribution of input X2 is known by the optimizer.

Example	Unknowns	Knowns	X1	X2	Output 1	Output 2
1	1	0	k_{MAP}	-	P_{maxLV}	-
2	1	1	k_{MAP}	Sf_{act}	P_{maxLV}	-
3	2	0	k_{MAP}	k_{LV}	P_{maxLV}	EDV_{LV}

3.6 Synthetic Examples

Before using the proposed framework to solve a real problem, it is tested with some synthetic examples where the input distribution is known a priori. Starting with the reference CircAdapt model configuration, we assume an input distribution or set of distributions and run a forward model to calculate any output metric CDFs. The goal is to find an input parameterization that accurately reproduces the calculated CDF. We can then check how closely the resulting input parameterization matches the input used in the forward model; recovering the initial input implies uniqueness of the solution. By using a synthetic input distribution to find the target CDFs, we know the optimization problem is solvable. These input distributions are truncated at $p = 0.01$ and $p = 0.99$, to ensure that the distribution can be recovered exactly.

Three synthetic problems were solved to test the DUU framework (Table 3.2). The first uses one probabilistic input to generate one target CDF, while all other variables are known and deterministic. The second adds a known probabilistic input which influences the same output. This shows how the method handles interactions between probabilistic variables. The third example uses two unknown probabilistic inputs to determine two probabilistic outputs. In this case, each input primarily influences a different output, but there are interaction effects between the two; this demonstrates optimization stability in multi-dimensional problems. Convergence studies of variable parameterization were performed for Examples 1 and 2.

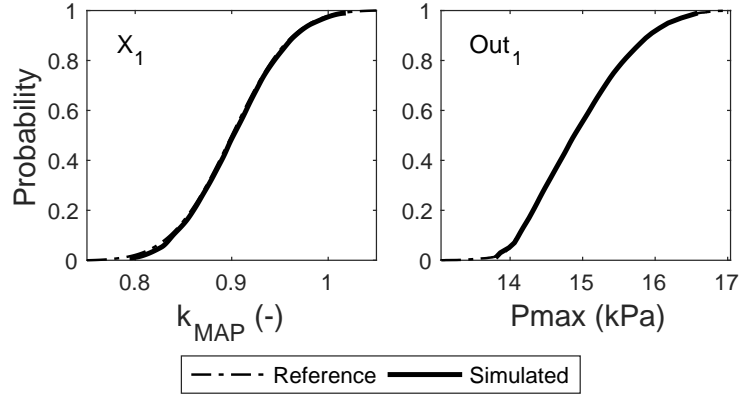


Figure 3.4 Results of Example 1.

3.6.1 Example 1: One unknown probabilistic variable

The first synthetic problem involves one unknown probabilistic variable and a single probabilistic output metric. The variable used is k_{MAP} ($\mu = 0.9$, $\sigma = 0.05$), which directly affects Pmax_{LV} . Figure 3.4 shows the tuned result, while Figure 3.5 shows the convergence with increasing values of N . Table 3.3 shows the RMS errors from the convergence study.

Table 3.3 Convergence results of iCDFs for Example 1.

N	X1		Output 1	
	Variable	RMSE	Metric	RMSE (kPa)
10	k_{MAP}	3.4e-3	Pmax_{LV}	2.78e-5
20	k_{MAP}	3.1e-3	Pmax_{LV}	1.57e-5
40	k_{MAP}	3.0e-3	Pmax_{LV}	1.26e-5

3.6.2 Example 2: One unknown and one known probabilistic variable

The second example adds a known probabilistic input. The newly introduced variable is Sf_{act} ($\mu = 1.344$ kPa, $\sigma = 0.036$ kPa), which also affects Pmax_{LV} . Figure 3.6 shows the

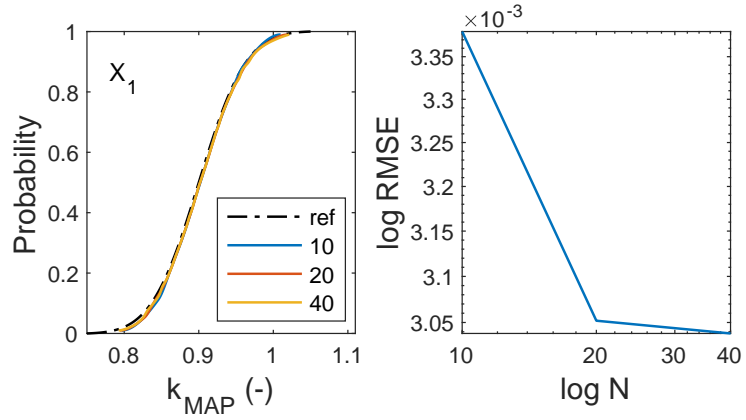


Figure 3.5 Convergence of resulting input CDFs from Example 1.

tuned result, while Figure 3.7 shows the convergence with increasing values of N . Table 3.4 shows the RMS errors from the convergence study.

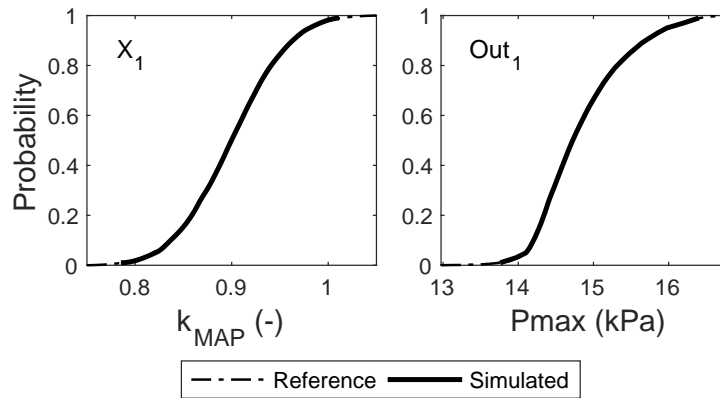


Figure 3.6 Results of Example 2.

3.6.3 Example 3: Two unknown probabilistic variables and two probabilistic outputs

The final example involves two unknown probabilistic input variables that primarily drive two separate model outputs. The input-output pairing of k_{MAP} and P_{maxLV} is the

Table 3.4 Convergence results of iCDFs for Example 2. The distribution of X2 is exactly known by the optimizer.

N	X1	Output 1		
	Variable	RMSE	Metric	RMSE
		-		(kPa)
10	k_{MAP}	28.0e-4	$P_{\text{max}_{\text{LV}}}$	25.8e-6
20	k_{MAP}	9.7e-4	$P_{\text{max}_{\text{LV}}}$	8.5e-6
40	k_{MAP}	6.2e-4	$P_{\text{max}_{\text{LV}}}$	2.0e-6

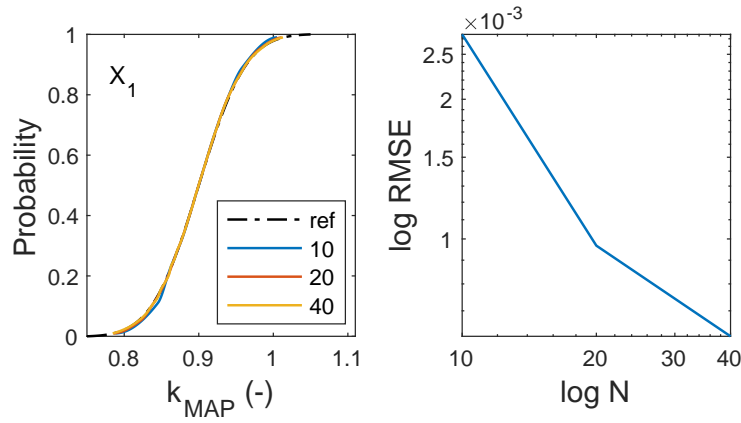


Figure 3.7 Convergence of resulting input CDFs from Example 2.

same as in Example 1. Now, the geometry scaling variable k_{LV} ($\mu = 1.05$, $\sigma = 0.01$) is added, which influences EDV_{LV} . Both inputs influence both outputs, so there is some cross-over effect in the optimization. Figure 3.8 shows the tuned result, while Figure 3.9 shows the effect of increasing values of N .

3.7 A Real-World Problem Using Patient Data

In the real-world, model input distributions are not known a priori. To simulate this, we again use the same combination of variables and outputs as in Example 3, but we now describe Gaussian target CDFs directly using patient and reference data. The mean for these CDFs is the value obtained from the patient, while the standard deviation comes

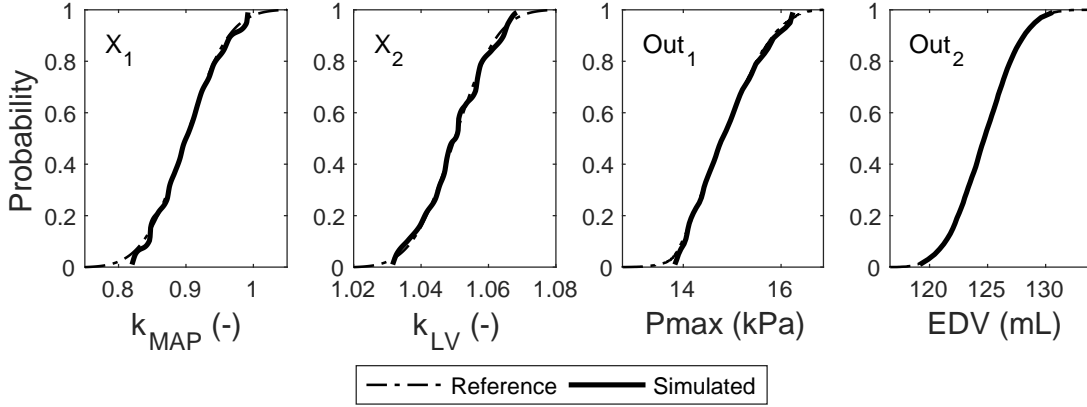


Figure 3.8 Results of Example 3.

from documented measurement errors in the literature (Ribezzo et al., 2014; Gordon et al., 1983). Figure 3.10 shows the tuned result, while Table 3.5 shows the resulting RMS errors.

Table 3.5 Results for the Real-World example.

Output 1		Output 2	
Metric	RMSE	Metric	RMSE
	(kPa)		(mL)
Pmax _{LV}	5.68e-6	EDV _{LV}	2.04e-4

3.8 Discussion

Our results show that the proposed framework reliably discovered distributions of input parameters which accurately reproduce target output distributions. All four of the studied tuning examples resulted in reasonable input distributions. The three synthetic examples demonstrated that the the approach works with multiple probabilistic inputs, whether one or more of those inputs are being tuned. Accurate reproduction of the original input distributions in those examples also exhibits consistency and reliability of the tuned result.

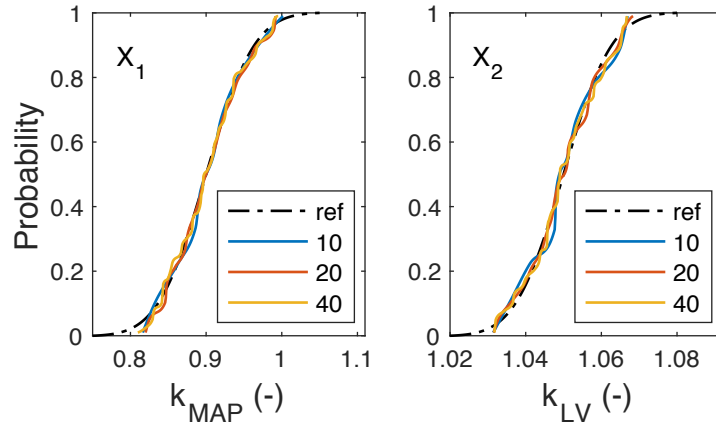


Figure 3.9 Variation of input CDFs from Example 3 with increasing values of N .

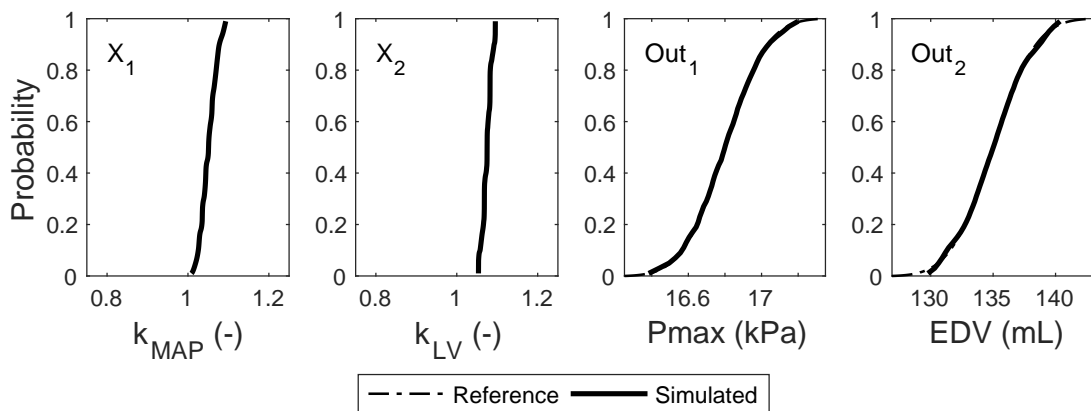


Figure 3.10 Resulting input and output CDFs from a two-dimensional real-world problem, where both probabilistic inputs are tuned and do not have prior-known solutions. The bounds of the plots of x_1 and x_2 represent the bounds of the surrogate.

The real-world PSM problem was solved with the use of patient data, further proving the stability of the framework in non-idealized model configurations.

An unexpected discovery during testing of the framework was that many implementations of probabilistically-uniform CDF sampling will introduce errors caused by false correlation when extended to multiple input variables. This is because the nature of the CDF causes sample values to be monotonic. Randomization was initially used to combine sample vectors, but this causes the optimization objective to become stochastic - preventing convergence to a precise optima. The final implementation of multi-variable sampling, using the tensor product, was selected due to this need for a deterministic sampling approach.

While our method was designed and tested to work with a broad range of models and domains, there are still a few key limitations related directly to the tuned inputs. While the algorithm was able to generate very good solutions for all examples shown, based on the objective functions we defined, there is no computationally-tractable way to prove that the solutions found are unique. This means that there may be other input distributions that equally satisfy our objective, or produce a similar quality output distribution. Similarly, there is no guarantee of a global optimum, which means that a better solution to the chosen objective may exist. For these reasons, there will always be some potential for the tuned distributions to arbitrarily differ from measurable values of the real-world modeled system.

Other limitations of the framework are inherent to the use of the surrogate. Though the surrogate provides many benefits in terms of computational-efficiency and robustness, it introduces the potential for divergence from the original model. The model sampling used to build the surrogates for the studied examples were very dense, but it is difficult to define the maximum error in the same units as the modeled output. This makes it impossible to make any guarantees on the upper bound of inaccuracy at any unsampled location on the surrogate. However, the surrogate will be exactly accurate at each sampled location and some region surrounding it. Another limitation is that the bounds of the surrogate must be

predetermined when it is generated. The issue with this is that it can be difficult to know what value ranges will be needed to capture extreme tails of input distributions.

To summarize, the proposed framework enables further automation of model tuning with uncertain data, increasing utility of computerized models in domains where reliable data is expensive or unavailable. The use of a surrogate makes the methodology computationally efficient, which allows even expensive models to be tuned in such environments. Our results from tuning the CircAdapt model support the applicability of this tool for PSM in a clinical setting with non-idealized inputs. This approach also has potential applications in broader problems of model design.

3.9 References

- Arts, T., Delhaas, T., Bovendeerd, P., Verbeek, X., and Prinzen, F. W. (2005). Adaptation to mechanical load determines shape and properties of heart and circulation: the CircAdapt model. *American Journal of Physiology: Heart and Circulatory Physiology*, 288:H1943–H1954.
- Clay, S., Alfakih, K., Radjenovic, A., Jones, T., Ridgway, J. P., and Sinvananthan, M. U. (2006). Normal range of human left ventricular volumes and mass using steady state free precession MRI in the radial long axis orientation. *Magnetic Resonance Materials in Physics, Biology and Medicine*, 19(1):41–45.
- Cressie, N. (1988). Spatial prediction and ordinary kriging. *Mathematical geology*, 20(4):405–421.
- De Boor, C. and Ron, A. (1990). On multivariate polynomial interpolation. *Constructive Approximation*, 6(3):287–302.
- Dyn, N., Levin, D., and Rippa, S. (1986). Numerical procedures for surface fitting of scattered data by radial functions. *SIAM Journal on Scientific and Statistical Computing*, 7(2):639–659.
- Ellwein, L. M., Pope, S. R., Xie, A., Batzel, J., Kelley, C. T., and Olufsen, M. S. (2013). Modeling cardiovascular and respiratory dynamics in congestive heart failure. *Mathematical Biosciences*, 241:56–74.
- Fang, H. and Horstemeyer, M. F. (2006). Global response approximation with radial basis functions. *Engineering Optimization*, 38(04):407–424.
- Friedman, J. H. (1991). Multivariate adaptive regression splines. *The annals of statistics*, pages 1–67.

- Gordon, E. P., Schnittger, I., Fitzgerald, P. J., Williams, P., and Popp, R. L. (1983). Reproducibility of left ventricular volumes by two-dimensional echocardiography. *Journal of the American College of Cardiology*, 2(3):506–513.
- Huberts, W., Heinen, S. G., Zonnebeld, N., van den Heuvel, D. A., de Vries, J. P. P., Tordoir, J. H., Hose, D. R., Delhaas, T., and van de Vosse, F. N. (2018). What is needed to make cardiovascular models suitable for clinical decision support? A viewpoint paper. *Journal of Computational Science*, 24:68–84.
- Iman, R. L. and Helton, J. C. (1988). An Investigation of Uncertainty and Sensitivity Analysis Techniques for Computer Models. *Risk Analysis*, 8(1):71–90.
- Kerckhoffs, R. C. P., Lumens, J., Vernoooy, K., Omens, J. H., Mulligan, L. J., Delhaas, T., Arts, T., McCulloch, A. D., and Prinzen, F. W. (2008). Cardiac resynchronization: Insight from experimental and computational models. *Progress in Biophysics and Molecular Biology*, 97(2-3):543–561.
- Krishnamurthy, A., Villongco, C. T., Chuang, J., Frank, L. R., Nigam, V., Belezzuoli, E., Stark, P., Krummen, D. E., Narayan, S., Omens, J. H., McCulloch, A. D., and Kerckhoffs, R. C. P. (2013). Patient-specific models of cardiac biomechanics. *Journal of Computational Physics*, 244:4–21.
- Kuikka, J., Lehtovirta, P., Kuikka, E., and Rekonen, A. (1974). Application of the modified gamma function to the calculation of cardiopulmonary blood pools in radiocardiography. *Physics in Medicine and Biology*, 19(5):692–700.
- Leifsson, L., Koziel, S., and Kurgan, P. (2014). Automated low-fidelity model setup for surrogate-based aerodynamic optimization. In *Solving Computationally Expensive Engineering Problems*, pages 87–111. Springer.
- MathWorks (2017). MATLAB R2017b.
- Mineroff, J., McCulloch, A. D., Krummen, D., and Krishnamurthy, G. A. (2018). Optimization Framework for Patient-Specific Cardiac Modeling. *Submitted to Biomechanics and Modeling in Mechanobiology*.
- Neal, M. L. and Kerckhoffs, R. (2009). Current progress in patient-specific modeling. *Briefings in Bioinformatics*, 11(1):111–126.
- Niederer, S. A., Fink, M., Noble, D., and Smith, N. P. (2009). A meta-analysis of cardiac electrophysiology computational models. *Experimental Physiology*, 94(5):486–495.
- Pokuri, B. S. S., Lofquist, A., and Ganapathysubramanian, B. (2018). Paryopt: Parallel asynchronous remote bayesian optimization. *Submitted to ACM transactions on Mathematical Software*.

- Raamat, R., Talts, J., Jagomägi, K., and Kivastik, J. (2013). Accuracy of some algorithms to determine the oscillometric mean arterial pressure: A theoretical study. *Blood Pressure Monitoring*, 18:50–56.
- Reinbolt, J. A., Haftka, R. T., Chmielewski, T. L., and Fregly, B. J. (2008). A computational framework to predict post-treatment outcome for gait-related disorders. *Medical Engineering and Physics*, 30:434–443.
- Ribezzo, S., Spina, E., Di Bartolomeo, S., and Sanson, G. (2014). Noninvasive techniques for blood pressure measurement are not a reliable alternative to direct measurement: A randomized crossover trial in ICU. *The Scientific World Journal*, 2014.
- Robinson, T., Eldred, M., Willcox, K., and Haimes, R. (2008). Surrogate-based optimization using multifidelity models with variable parameterization and corrected space mapping. *Aiaa Journal*, 46(11):2814–2822.
- Roth, G. A., Huffman, M. D., Moran, A. E., Feigin, V., Mensah, G. A., Naghavi, M., and Murray, C. J. L. (2015). Global and regional patterns in cardiovascular mortality from 1990 to 2013. *Circulation*, 132(17):1667–1678.
- Sankaran, S. and Marsden, A. L. (2011). A Stochastic Collocation Method for Uncertainty Quantification and Propagation in Cardiovascular Simulations. *Journal of Biomedical Engineering*, 133(March 2011):1–12.
- Shortliffe, E. H., Buchanan, B. G., and Feigenbaum, E. A. (1979). Knowledge engineering for medical decision making: A review of computer-based clinical decision aids. Technical report, Stanford University Computer Science Department.
- Walker, W., Rotmans, J., and Janssen, P. (2003). Defining Uncertainty : A Conceptual Basis for Uncertainty Management in Model-Based Decision Support A Conceptual Basis for Uncertainty Management in Model-Based Decision Support. *Integrated Assessment*, 4(1):5–17.
- Xiu, D. and Sherwin, S. J. (2007). Parametric uncertainty analysis of pulse wave propagation in a model of a human arterial network. *Journal of Computational Physics*, 226:1385–1407.

CHAPTER 4. SUMMARY AND CONCLUSION

This framework can facilitate the widespread use of patient-specific or subject-specific models by enabling tuning from non-invasive data. The proposed approach enables further automation of model tuning with uncertain data, increasing utility of computerized models in domains where reliable data is expensive or unavailable. The optimization methods employed are resource efficient and easily scalable to the needs and computational capacity of the application. The use of a surrogate makes the methodology computationally efficient, which allows even expensive models to be tuned in such environments.

Using an optimization framework, the information learned in the medical community can be easily and reliably distributed, making it relatively easy to tune a new patient model in a clinical environment compared with current manual methods. The framework is also usable in a research setting, where a major concern is maintaining a consistent protocol in cross-species research. By tuning both human and canine circulatory models with no modifications to the implementation besides reference parameter values, it was demonstrated that this concern can be naturally addressed. The application of this work in cross-species research can contribute to improved treatment of CVD. There are also potential applications in broader problems of model design.

Though the proposed framework addressed many of the issues currently impeding the use of patient-specific cardiovascular models, there are still some key limitations to its application. The first is that the use of noninvasive data imposes limitations on accuracy and data acquisition. However, requiring invasive procedures reduces the value of the framework as compared to more traditional explorative methodologies. The most efficient response is

to determine the data sources which are most sensitive and justify the most effort to capture accurately. UQ can then be used to mitigate the resulting decision uncertainty.

Additionally, while the algorithm was able to generate very good solutions for all examples shown based on the objective functions we defined, there is no computationally-tractable way to prove that the solutions found are unique. This means that there may be other input distributions that equally satisfy our objective, or produce a similar quality output distribution. Similarly, there is no guarantee of a global optimum, which means that a better solution to the chosen objective may exist. For these reasons, there will always be some potential for the tuned values or distributions to arbitrarily differ from measurable values of the real-world modeled system.

Other limitations of the framework are inherent to the surrogate. Though meta-models provide many benefits in terms of computational-efficiency and robustness, they introduce the potential for divergence from the original model. The model sampling used to build the surrogates for the studied examples were very dense, but it is difficult to define the maximum error in the same units as the modeled output. This impedes guarantees on the upper bound of inaccuracy at any unsampled location on the surrogate. Another limitation is that the bounds of the surrogate must be predetermined when it is generated. The issue with this is that it can be difficult to know what value ranges will be needed to capture extreme tails of input distributions.

This work could be further developed in a number of directions. One interesting addition would be a tolerance for surrogate building. This would allow surrogate construction to stop when it is good enough instead of requiring the potentially excessive number of evaluations currently needed to expect accuracy over a broad domain. Specific to the domain of PSM, there is also the potential to use objectives more directly related to physiology.

In summary, this work lays the initial foundation of an automated optimization framework for patient-specific modeling with uncertainty quantification that could be applied in a clinical setting to improve patient treatment and, most importantly, outcomes. It can

also be used more broadly to support cross-species medical studies leading to more effective treatment options. Development of tools such as the proposed framework, along with increasingly complex models, will substantially increase our understanding of diseases and, thus, the standard of available medical care.

REFERENCES

- Agoshkov, V., Quarteroni, A., and Rozza, G. (2006). A mathematical approach in the design of arterial bypass using unsteady Stokes equations. *Journal of Scientific Computing*, 28(2-3):139–165.
- Baillargeon, B., Rebelo, N., Fox, D. D., Taylor, R. L., and Kuhl, E. (2014). The Living Heart Project: A robust and integrative simulator for human heart function. *European Journal of Mechanics - A/Solids*, 48:38–47.
- Dugdale, D. C., Epstein, R., and Pantilat, S. Z. (1999). Time and the Patient-Physician Relationship. *Journal of General Internal Medicine*, 14(Supplement 1):S34–S40.
- Ellwein, L. M., Pope, S. R., Xie, A., Batzel, J., Kelley, C. T., and Olufsen, M. S. (2013). Modeling cardiovascular and respiratory dynamics in congestive heart failure. *Mathematical Biosciences*, 241:56–74.
- Ferrario, M., Chiodini, P., Chambless, L. E., Cesana, G., Vanuzzo, D., Panico, S., Sega, R., Pilotto, L., Palmieri, L., and Giampaoli, S. (2005). Prediction of coronary events in a low incidence population. Assessing accuracy of the CUORE Cohort Study prediction equation. *International Journal of Epidemiology*, 34:413–421.
- Fuchs, V. R. and Milstein, A. (2011). The \$640 Billion Question - Why Does Cost-Effective Care Diffuse So Slowly? *New England Journal of Medicine*, 364(21):1985–1987.
- Gaziano, T. A., Steyn, K., Cohen, D. J., Weinstein, M. C., and Opie, L. H. (2005). Cost-effectiveness analysis of hypertension guidelines in South Africa: Absolute risk versus blood pressure level. *Circulation*, 112:3569–3576.
- Hendel, R. C., Patel, M. R., Allen, J. M., Min, J. K., Shaw, L. J., Wolk, M. J., Douglas, P. S., Kramer, C. M., Stainback, R. F., Bailey, S. R., Doherty, J. U., and Brindis, R. G. (2013). Appropriate use of cardiovascular technology. *Journal of the American College of Cardiology*, 61(12):1305–1317.
- Huberts, W., Heinen, S. G., Zonnebeld, N., van den Heuvel, D. A., de Vries, J. P. P., Tordoir, J. H., Hose, D. R., Delhaas, T., and van de Vosse, F. N. (2018). What is needed to make cardiovascular models suitable for clinical decision support? A viewpoint paper. *Journal of Computational Science*, 24:68–84.

- Krishnamurthy, A., Villongco, C. T., Chuang, J., Frank, L. R., Nigam, V., Belezzuoli, E., Stark, P., Krummen, D. E., Narayan, S., Omens, J. H., McCulloch, A. D., and Kerckhoffs, R. C. P. (2013). Patient-specific models of cardiac biomechanics. *Journal of Computational Physics*, 244:4–21.
- Landrigan, C. P., Parry, G. J., Bones, C. B., Hackbarth, A. D., Goldmann, D. A., and Sharek, P. J. (2010). Temporal Trends in Rates of Patient Harm Resulting from Medical Care. *New England Journal of Medicine*, 363(22):2124–2134.
- Leong, X. F., Ng, C. Y., and Jaarin, K. (2015). Animal Models in Cardiovascular Research: Hypertension and Atherosclerosis. *BioMed Research International*, 2015.
- Lim, E., Dokos, S., Lovell, N. H., Cloherty, S. L., Salamonsen, R. F., Mason, D. G., and Reizes, J. A. (2010). Parameter-Optimized Model of Cardiovascular-Rotary Blood Pump Interactions. *IEEE Transactions on Biomedical Engineering*, 57(2):254–266.
- Maddox, T. M., Chan, P. S., Spertus, J. A., Tang, F., Jones, P., Ho, P. M., Bradley, S. M., Tsai, T. T., Bhatt, D. L., and Peterson, P. N. (2014). Variations in coronary artery disease secondary prevention prescriptions among outpatient cardiology practices: Insights from the NCDR (National Cardiovascular Data Registry). *Journal of the American College of Cardiology*, 63(6):539–546.
- Marsden, A. L., Feinstein, J. A., and Taylor, C. A. (2008). A computational framework for derivative-free optimization of cardiovascular geometries. *Computer Methods in Applied Mechanics and Engineering*, 197(21-24):1890–1905.
- Mehta, R. H., Peterson, E. D., and Califf, R. M. (2007). Performance Measures Have a Major Effect on Cardiovascular Outcomes: A Review. *American Journal of Medicine*, 120:398–402.
- Milani-Nejad, N. and Janssen, P. M. L. (2014). Small and large animal models in cardiac contraction research: advantages and disadvantages. *Pharmacology and Therapeutics*, 141(3):235–249.
- Mozaffarian, D., Benjamin, E. J., Go, A. S., Arnett, D. K., Blaha, M. J., Cushman, M., Das, S. R., Ferranti, S. D., Després, J. P., Fullerton, H. J., Howard, V. J., Huffman, M. D., Isasi, C. R., Jiménez, M. C., Judd, S. E., Kissela, B. M., Lichtman, J. H., Lisabeth, L. D., Liu, S., MacKey, R. H., Magid, D. J., McGuire, D. K., Mohler, E. R., Moy, C. S., Muntner, P., Mussolino, M. E., Nasir, K., Neumar, R. W., Nichol, G., Palaniappan, L., Pandey, D. K., Reeves, M. J., Rodriguez, C. J., Rosamond, W., Sorlie, P. D., Stein, J., Towfighi, A., Turan, T. N., Virani, S. S., Woo, D., Yeh, R. W., and Turner, M. B. (2015). *Heart disease and stroke statistics - 2016 update: a report from the American Heart Association*, volume 133.
- Neal, M. L. and Bassingthwaite, J. B. (2007). Subject-specific Model Estimation of Cardiac Output and Blood Volume During Hemorrhage. *Cardiovascular Engineering*, 7(3):97–120.

- Porter, M. E. (2010). What Is Value in Health Care? *New England Journal of Medicine*, 363(26):2477–2481.
- Probst, M., Lüllesmann, M., Nicolai, M., Bücker, H. M., Behr, M., and Bischof, C. H. (2010). Sensitivity of optimal shapes of artificial grafts with respect to flow parameters. *Computer Methods in Applied Mechanics and Engineering*, 199(17-20):997–1005.
- Sankaran, S., Humphrey, J. D., and Marsden, A. L. (2013). An efficient framework for optimization and parameter sensitivity analysis in arterial growth and remodeling computations. *Computer Methods in Applied Mechanics and Engineering*, 256(1):200–210.
- Sankaran, S. and Marsden, A. L. (2011). A Stochastic Collocation Method for Uncertainty Quantification and Propagation in Cardiovascular Simulations. *Journal of Biomedical Engineering*, 133(March 2011):1–12.
- Shortliffe, E. H., Buchanan, B. G., and Feigenbaum, E. A. (1979). Knowledge engineering for medical decision making: A review of computer-based clinical decision aids. Technical report, Stanford University Computer Science Department.
- The World Bank (2012). World Development Indicators. Technical report.
- Vukanovic-Criley, J. M., Criley, S., Warde, C. M., Boker, J. R., Guevara-Matheus, L., Churchill, W. H., Nelson, W. P., and Criley, J. M. (2006). Competency in cardiac examination skills in medical students, trainees, physicians, and faculty: a multicenter study. *Archives of internal medicine*, 166(6):610–616.
- Wilson, P. W. F., D’Agostino, R. B., Levy, D., Belanger, A. M., Silbershatz, H., and Kannel, W. B. (1998). Prediction of coronary heart disease using risk factor categories. *Circulation*, 97:1837–1847.
- World Health Organization (2008). The Global Burden of Disease: 2004 update. Technical report.